Biophysical Reviews (2020) 24:65–84
https://doi.org/10.1007/s12551-020-00620-9

REVIEW

Urea-aromatic interactions in biology

Shampa Raghunathan[1] · **Tanashree Jaganade**[1] · **U. Deva Priyakumar**[1]

Received: 5 December 2019 / Accepted: 8 January 2020 / Published online: 17 February 2020

Abstract

Noncovalent interactions are key determinants in both chemical and biological processes. Among such processes, the hydrophobic interactions play an eminent role in folding of proteins, nucleic acids, formation of membranes, protein-ligand recognition, etc.. Though this interaction is mediated through the aqueous solvent, the stability of the above biomolecules can be highly sensitive to any small external perturbations, such as temperature, pressure, pH, or even cosolvent additives, like, urea—a highly soluble small organic molecule utilized by various living organisms to regulate osmotic pressure. A plethora of detailed studies exist covering both experimental and theoretical regimes, to understand how urea modulates the stability of biological macromolecules. While experimentalists have been primarily focusing on the thermodynamic and kinetic aspects, theoretical modeling predominantly involves mechanistic information at the molecular level, calculating atomistic details applying the force field approach to the high level electronic details using the quantum mechanical methods. The review focuses mainly on examples with biological relevance, such as (1) urea-assisted protein unfolding, (2) urea-assisted RNA unfolding, (3) urea lesion interaction within damaged DNA, (4) urea conduction through membrane proteins, and (5) protein-ligand interactions those explicitly address the vitality of hydrophobic interactions involving exclusively the urea-aromatic moiety.

Keywords Molecular dynamics simulations · Aromatic · Amino acids · Stacking interactions · QM calculations · Urea · RNA · DNA · Nucleic acids · Urea transporter

Introduction

Biological macromolecules, such as proteins and nucleic acids, are integral part of living organisms. Recent advances in both experimental methods and computer simulations have essentially shown that hydrophobic interactions greatly assist their biological functions. Though these interactions in proteins are typically mediated through aqueous solvent, small changes in temperature, pressure, and pH or by changing the composition of the added cosolvents to the solution can cause the biologically active native state (which is only marginally stable in its folded form Wales (2003)) to denature to form an inactive unfolded state. Such a cosolvent, urea—a highly hydrophilic small organic molecule—plays a central role in the physiological processes of bacteria (Godara et al. 2009), mammals (LeMoine and Walsh 2015), etc.. While urea serves as a nitrogen source for bacteria (Sebbane et al. 2002; Levin et al. 2009), it controls the osmotic pressure and aids in water reabsorption in the mammalian kidney (Esteva-Font et al. 2015; Levin et al. 2012). Urea can also have indirect effects, via protein carbamoylation (Delanghe et al. 2017). Carbamoylation-derived products, such as carbamoylated albumin, carbamoylated hemoglobin (cHb), and carbamoylated low-density lipoprotein (cLDL), are produced by the reaction of proteins, peptides, or amino acids with isocyanic acid which is formed due to the deamination of urea. Carbamoylation can have different pathophysiological effects. Given the widespread activity of urea in biology, a detailed study is essential in order to understand their biological functions.

This is a review of work focused on noncovalent interactions of urea and urea moieties with primarily amino acids—phenylalanine (Phe), tyrosine (Tyr), tryptophan (Trp), and Histidine (HIS)— and the RNA nucleobases—adenine (ADE), guanine (GUA), cytosine (CYT), and uracil

✉ U. Deva Priyakumar
deva@iiit.ac.in

[1] Center for Computational Natural Sciences and Bioinformatics, International Institute of Information Technology, Hyderabad, 500032, India

(URA)—all of which have aromatic groups. The sheer volume of research aimed at investigating such phenomena is evidence of the vast importance of this topic. A review, such as this, cannot capture the full extent of available information in every facet of biological sciences that utilizes this knowledge. Instead, here we contribute a compilation of those systems, where urea-aromatic hydrophobic interactions are of great biological relevance: (1) urea-assisted protein unfolding, (2) urea-assisted RNA unfolding, (3) urea lesion incorporated DNA, (4) urea conduction through membrane proteins, and (5) protein-ligand interactions. Accordingly, investigations aimed at an energetic and structural quantification of individual interactions with aromatic rings in biological complexes are reviewed. Experimental and theoretical approaches starting from force fields to high-level quantum mechanical computational studies are discussed.

Each section begins with an emerging view of a particular research topic based on their impact on developing the field, focusing specifically on advancements in the past few years. Finally, we discuss how greater knowledge of urea-aromatic interactions would be of significant importance for improved lead optimization and drug design.

Urea-assisted protein unfolding

Urea-assisted denaturation of proteins has been extensively used to investigate protein stability and folding phenomenon both experimentally and computationally (Kauzmann 1959; Pace 1986; England and Haran 2011; England et al. 2008; Canchi and García 2013; Bandyopadhyay et al. 2014). In a recent review, Hall et al. re-examined the site-binding model of protein originally proposed by Schellman (1955a, b) and Tanford (Aune and Tanford 1969), which essentially considered the effective concentration of a denaturant interacting with protein (Hall et al. 2018). Owing to the recent advances, in both experimental and computer simulations methods, we have been gaining a deeper understanding of protein folding mechanisms (Holehouse et al. 2015; Cheng et al. 2017; Guinn et al. 2011, 2015; Goyal et al. 2017). The scientific community was divided in terms of the mechanistic viewpoint on urea-induced protein denaturation.

In the indirect mechanism (Rupley 1964; Frank and Franks 1968; Finer et al. 1972; Hoccart and Turrell 1993; Granick and Bae 2008; Bandyopadhyay et al. 2014; Bellissent-Funel et al. 2016), in presence of urea (as cosolvent), the water structure is disrupted; hence, the hydrophobic effect becomes weaker within the protein which is the major driving force for protein unfolding. However, earlier experimental and computational data are somewhat ambiguous on the effect of urea on water structure. In some studies, urea is suggested to disrupt the water structure, and termed as a water-"structure breaker" (Finer et al. 1972; Hoccart and Turrell 1993). Others hypothesized that urea enhanced the water structure and coined the term as "structure maker" (Vanzi et al. 1998; Chitra and Smith 2000). Both these two views attribute the peculiarities and uncertainties at certain level which tell us that affecting the water structure cannot be the sole effect of urea towards denaturing a protein.

On the contrary, according to the direct mechanism, urea locally interacts with protein rather than impacting the water network resulting in changes in the global landscape of the protein. Protein is an amino acid heteropolymer with a unique (for each protein) sequence (Finkelstein and Galzitskaya 2004; Onuchic et al. 1997); its chemically complex construct is made of peptide backbone and side chains which can have polar, apolar, or charged variants. Scientists have spent decades to find whether side chain or backbone or even both have dominant contributions in urea-protein interactions as well as their nature of interaction. In this regard, mechanistic inferences from the past studies have been rather divergent: Some experimental and theoretical studies showed that side chains have greater contributions (O'Brien et al. 2007; Stumpe and Grubmüller 2007; 2008; 2009). While, a series of studies (Street et al. 2006; Auton and Bolen 2004; Auton et al. 2007, 2008; Bolen and Rose 2008) by Bolen and coworkers revealed that denaturing/protecting osmolytes are preferentially accumulated/excluded around the protein backbone in single-component osmolyte solutions using the transfer free energy (TFE) model originally proposed by Tanford (Tanford 1964). However, accessible surface area–based TFE model (Moeser and Horinek 2013) predicted that both the backbone and the side chain significantly contribute to the *m*-value and favor denaturation. This would indicate a stepwise denaturation process of protein by urea (Holehouse et al. 2015; Rossky 2008). Hua et al. observed that once urea has expelled the first hydration layer around the protein, the hydrophobic core is penetrated by urea before water, forming a "dry globule" (Hua et al. 2008). The direct mechanism is a coherent result of the favorable interaction of urea with all protein moieties, including the peptide backbone and the side chains to varying degrees (Hua et al. 2008; Horinek and Netz 2011; Stumpe and Grubmüller 2007; Lee et al. 2010; Guinn et al. 2011). Nevertheless, today, it is widely accepted that the chemical nature of the functional groups present in each amino acid strongly corroborates their contributions towards urea-protein interactions. Therefore, it is of great interest to elucidate the molecular basis of urea's effect on protein stability. These contemporary understanding of molecular forces involved in protein's local structure

helped to quantify their individual contribution towards urea-induced protein unfolding landscape globally.

MD simulations have been used extensively to examine the nature of urea-protein interactions. Studies were focused on diverse model amino acids as well as real proteins, e.g., small hydrophobic solutes (Stumpe and Grubmüller 2007; Moeser and Horinek 2013; Wallqvist et al. 1998; Shimizu and Chan 2002; Oostenbrink and van Gunsteren 2005; Lee and van der Vegt 2006; O'Brien et al. 2007), purely hydrophobic polymers (Auton and Bolen 2005; Zangi et al. 2009; Su and Dias 2017), and Trp-cage miniprotein (Canchi et al. 2010; Canchi and García 2011), lysozyme (Hua et al. 2008), and chymotrypsin inhibitor (Bennion and Daggett 2003). On the one hand, the fact that urea forms energetically favorable contacts with purely hydrophobic groups signifies that urea stabilizes the unfolded states. On the other hand, urea addition reduces the compactness of the polymer and urea's self-aggregation. This indicates that urea has a favorable dispersion interactions. Even, studies at a larger length scale, such as, unfolding of lysozyme protein infers the same effect that urea's dispersion interactions facilitate protein unfolding (Hua et al. 2008).

There are several prominent studies on the choice of the force fields to model the solute-cosolvent interactions in MD simulations (Horinek and Netz 2011; Canchi and García 2013; Ganguly et al. 2017)**.** Among such MD force fields, Kirkwood-Buff-derived force field (KBFF) (Weerasinghe and Smith 2003) and OPLS models (Duffy et al. 1993b) are commonly used for aqueous-urea solutions. In the case of interaction of urea with peptides and proteins (Goyal et al. 2017), the CHARMM general force field (CGenFF) (Vanommeslaeghe et al. 2010) for urea was shown to produce results in fairly good agreement with the KBFF. Here, transfer free energies obtained using the CHARMM-CGenFF agree well the with experimental data. In this study, authors have shown that various noncovalent urea-peptide binding interactions which were charaterized using the MD simulations, identified well with the state-of-the-art QM methods (see later).

Despite the relatively wide range of computational studies, experimental information is sparse concerning how urea molecules interact with different components of proteins on the atomic scale as these interactions can only be probed via techniques which measure on the order of angstroms (Steinke et al. 2016). In the 1960s on the basis of thermodynamics, the classical transfer model of Tanford (1970) assumed an unfolded ensemble that is independent of denaturant concentration. Also the pulse-field gradient nuclear magnetic resonance measurements by Wilkins et al. (1999), small angle X-ray scattering (SAXS) by Kohn et al. (2004), and fluorescence correlation spectroscopy (FCS) experiments by Holehouse et al. (2015) considered urea to populate heterogeneous conformational ensembles; single-molecule Förster resonance energy transfer (FRET) experiments (Merchant et al. 2007; Ziv and Haran 2009) predicted that the conformations in the denatured ensemble expose more surface areas as the concentration of the denaturant increases. As the accessible surface area due to the unfolding of protein upon urea addition changes, Guinn et al. 2011, 2015; Record et al. 2013 further measured the interaction of urea with a wide range of model compounds. They have used osmometry to characterize its interaction with various types of molecular surfaces of protein. Using the solute partitioning model (SPM), they reported urea accumulation in the vicinity of various functional groups of the protein in the following order: aromatic-C $\sim$ amide-O $>$ carboxyl-O $>$ amide-N $>$ hydroxyl-O $>$ aliphatic-C. In aqueous urea, while NH–π interactions have been realized to be the key mode of interaction, OH-π interactions involving water and aromatic groups are suitable to the same extent, and hence this does not justify the preferential interaction when it comes to water vs. urea. Recently, Cheng et al. (2017) examined the amide-aromatic interactions using osmometry and solubility measurements. They found that amide-O interaction is more favorable than amide-N interaction. However, atomistic details of the nature of interactions that lead to such a novel phenomenon of interaction between urea and aromatic groups were not known. Only recently, Goyal et al. (2017) have manifested the nature of urea-aromatic interactions, namely, π-π and NH-π stacking interactions which are of high relevance and importance in urea-assisted protein denaturation.

A variety of computational and experimental studies have been employed on Trp-cage miniprotein, a 20-residue

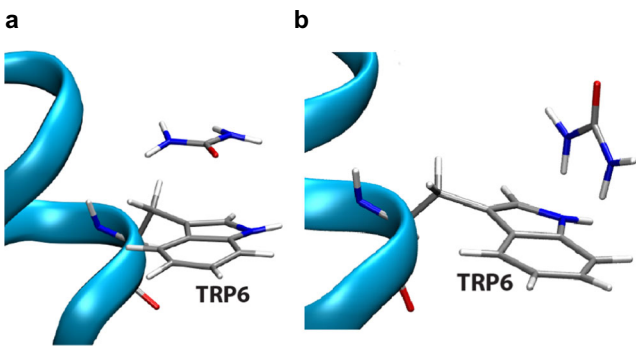

Fig. 1 Representative configurations of **a** Trp-urea stacking interaction and **b** Trp-urea NH$-\pi$ interaction. Adapted with permission from Goyal et al. (2017). Copyright (2017) American Chemical Society

polypeptide with a protein-like fold to study protein folding. Free energy profiles corresponding to the unfolding of the same in the presence and absence of urea at different temperatures identify the distortion of the hydrophobic core to be one of the essential steps (Goyal et al. 2017). In the presence of urea, the Trp6 residue which is of prime importance to the hydrophobic core becomes exposed to the solvent. As a result, the stabilization effect due to urea comes into play. Previous experiments reported that urea has a high affinity for aromatic groups of proteins. Naturally, the question arises what is the nature of the interaction between urea and aromatic groups of proteins. Goyal and co-workers have shown recently that urea can form stacking and NH-π interactions with aromatic groups of proteins (Fig. 1a and b for Trp-urea stacking and NH-π configurations, respectively). These novel interactions constitute an important aspect of urea's high affinity towards aromatic groups.

Insights from molecular dynamics simulations

Recognition of stacking and NH-π interactions:

Molecular dynamics (MD) simulations of Trp-cage miniprotein in the presence of urea were performed to describe and predict the geometry of interactions. To identify urea-aromatic stacking interactions involving urea and various aromatic groups, certain geometric criteria were used (exact details are given in ref. (Goyal et al. 2017)). Figure 2a shows the probability distributions of the two parameters, namely distance and angle between the Trp6 side chain and urea, calculated for the folded and unfolded states at 300 K. Here, urea-aromatic stacking interactions can readily be seen in case of unfolded states and not in folded states. The position of the highest peak in the probability distribution defines the closest contact between the two moieties. The probability distributions corresponding to the unfolded states exhibit a peak at a distance of 3.3 Å. Note that hydrogen bond–like contacts would exhibit a peak around 2.8 Å. Whereas, a cationic nucleobase was shown to be sandwiched at a distance of about 3.5 Å between two Trp side chains (Niedzwiecka et al. 2002). Similar, stacking-type interactions between the guanidinium group and aromatic side chains have been demonstrated before by Duffy et al. (1993a), Mason et al. (2004), Schug and Lindner (2005), and Mason et al. (2009). However, those were characterized as cation-π interactions (Meyer et al. 2003). The intermolecular interactions of urea molecules with the π-surface of the aromatic side chain via the N–H bond were analyzed. The probability distributions for the distance and angle parameters between the Trp6 side chain and urea (Fig. 2b) for the folded and unfolded states indicate the following: At distance of 3.3–3.4 Å, and angles in the range of 155–160° correspond to the most preferred orientations of urea with respect to the aromatic group for this type of interaction.

Having found that stacking and NH-π interactions are highly predominant in stabilizing Trp6 in unfolded states of Trp-minicage in the presence of urea, the authors were prompted towards postulating similar motifs, such as, other aromatic amino acids would as well be capable of forming stacking with urea. To this end, five model systems (benzene, phenol, indole, imidazole, and imidazolium ions, Fig. 3a) were conceived to examine urea stacking and NH-π interactions with all the aromatic residues. The interaction energies calculated relative to the interaction energies obtained for the pure water system are given in

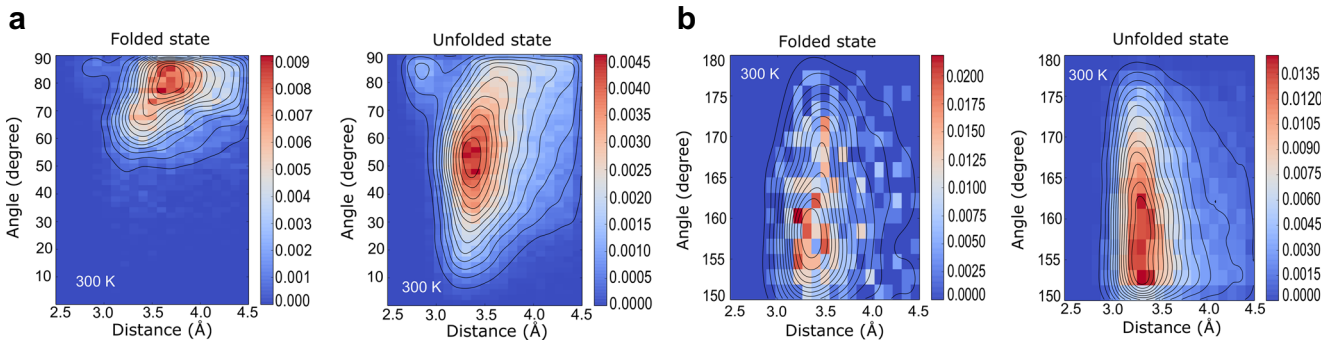

Fig. 2 Probability distributions of distance and angle parameters between the Trp6 side chain and urea, calculated for the folded and unfolded states at 300 K, in case of: **a** Trp-urea stacking interaction, and **b** Trp-urea NH−π interaction. Color bar represents normalized probability, such that, the sum of the values in each graph in the given range of distance and angle is unity. Adapted with permission from Goyal et al. (2017). Copyright (2017) American Chemical Society

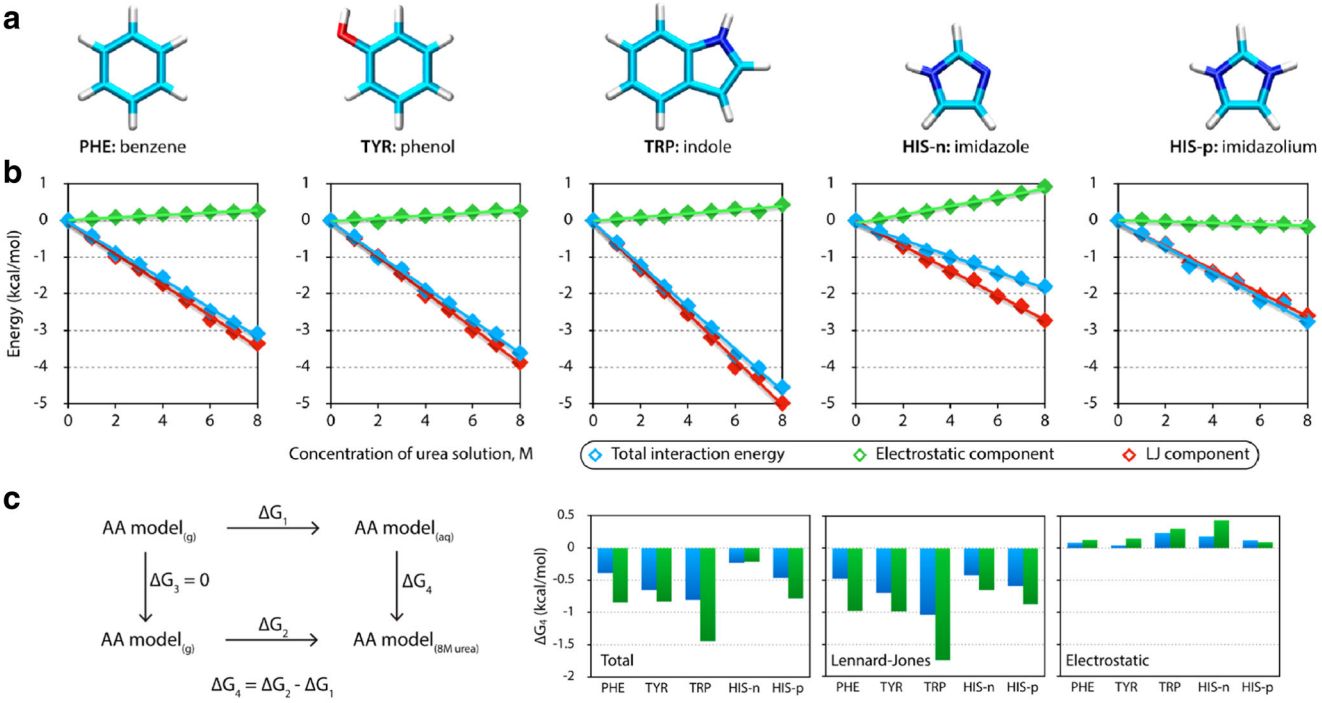

Fig. 3 Interaction energies and transfer free energies of five aromatic model systems with urea, used for MD simulations. **a** Representative models of five different aromatic side chains. **b** Interaction energies (blue) between model systems and solvent for 1–8 M urea solutions w.r.t. 0 M urea. Coulombic (green) and van der Waals (red) contributions to total interaction energies. **c** Thermodynamic cycle for calculating transfer free energies using thermodynamic integration method. Total free energies; and electrostatic and vdW contributions for 0 to 4 M (blue) and 0 to 8 M (green) urea solutions. Reprinted with permission from Goyal et al. (2017). Copyright (2017) American Chemical Society

Fig. 3b. In all the systems, interaction between the aromatic model compounds and the solvent is increasingly favorable due to the increase in concentration of urea, showing a linear dependence. The net stabilization owing to the presence of urea compared with the pure water system is mainly because of the favorable vdW-type dispersion interactions in all the systems. Similar to the interaction energies, the solvation free energies calculated using the thermodynamic integration method (Fig. 3c) of all the aromatic model systems become more favorable in the presence of urea due to the favorable vdW-type dispersion contributions, where the electrostatic contributions are marginally repulsive.

Quantum mechanical calculations

High-level ab inito quantum mechanical calculations at the RI-MP2/cc-pVDZ (Weigend et al. 1998; Dunning 1989) level of theory were performed on the aforementioned five model systems to validate MD results of stacking and NH-π interactions between urea and aromatic groups (Goyal et al. 2017). In fact, about a couple of hundreds of orientations of urea w.r.t. each model were considered for optimization. The most stable stacking and NH-π arrangement of urea-aromatic models are illustrated in Fig. 4a and b, respectively; additionally noncovalent interaction plots (NCI plots) showing weak interaction between the two interacting partners. Besides, potential energy surface (PES) calculations were carried out at the MP2/aug-cc-pVDZ level. Here, the two most stable complexes from each type of interactions were considered as the initial geometries. Figure 4c depicts the PESs for both of these, which shows well-defined minima corresponding to both stacking and NH-π interactions. The energy decomposition analysis of the QM interaction energy showed the dispersion contribution to be the favorable one, and not the electrostatic interaction. Thus, the results obtained using the MD simulations and the quantum mechanical calculations are consistent with each other, supporting the role of stacking and NH-π interactions in favoring the exposure of aromatic residues in the presence of urea.

Experimental evidence of urea-aromatic stacking interactions

Dougherty et al. (Ma and Dougherty 1997) were the first to outline cation-π interactions as one of the driving noncovalent forces used by nature in defining protein structures and protein-ligand interactions. Basically, they

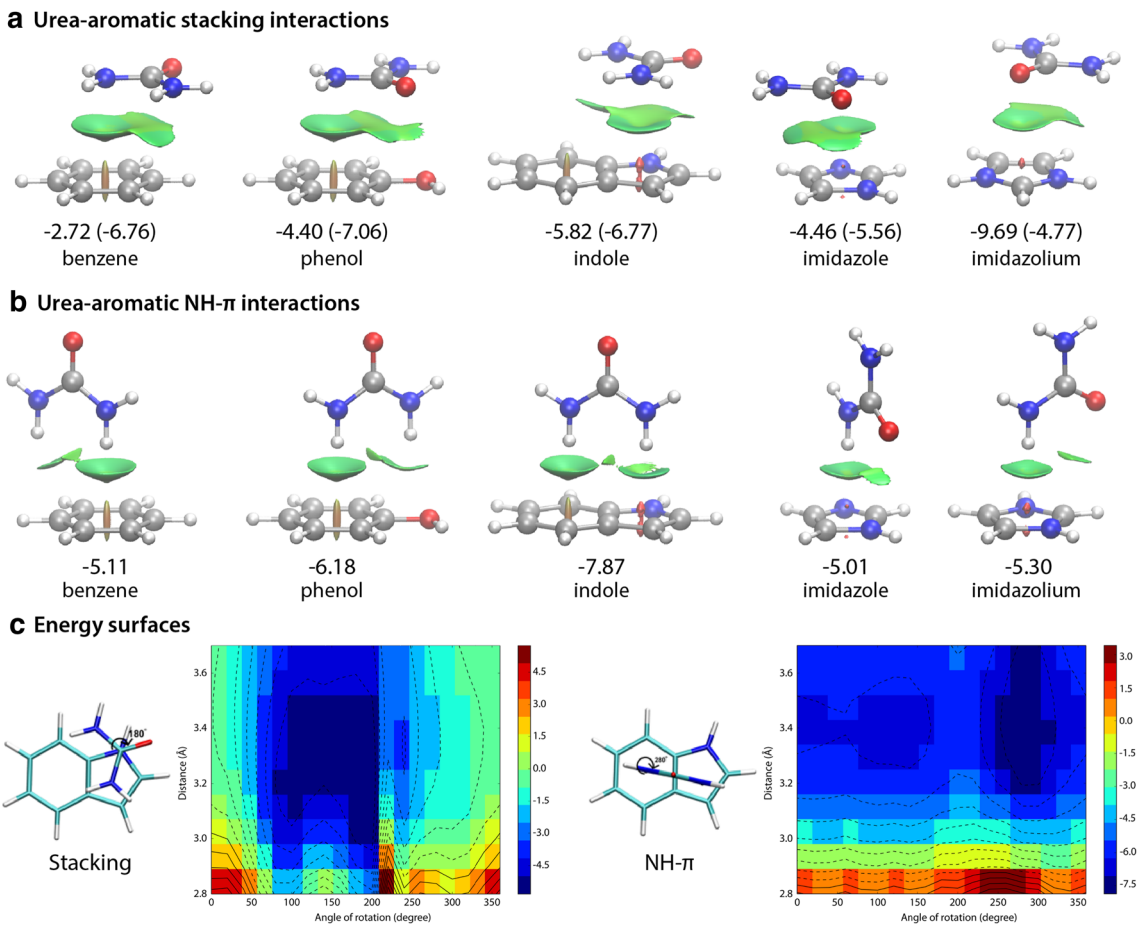

Fig. 4 Structures and energetics (kcal/mol) of urea-model pairs from QM calculations. **a** Most stable stacking arrangement. **b** Green-colored isosurfaces obtained from NCI plot showing a weak noncovalent interaction between the molecules. **c** Potential energy surfaces corresponding to the most stable stacking and NH$-\pi$ interactions obtained at the RI-MP2/aug-cc-pVDZ level. Interaction energies were calculated w.r.t. the distance between urea and indole, and the orientation of urea with respect to indole. Energy values are in kcal/mol. Reprinted with permission from Goyal et al. (2017). Copyright (2017) American Chemical Society

performed an investigation on modeling interactions found in the Protein Data Bank (PDB) with ab initio methods. Among structures surveyed, over 70% of the arginine side chains were found in the vicinity to an aromatic side chain; arginine was either perpendicular or parallel to the aromatic plane. Similarly, interactions between aromatic amino acid side chains are abundant in proteins, as shown by the pioneering work of Burley and Petsko (1985). They demonstrated, in a study involving 34 proteins, that on average, 60% of aromatic side chains (Phe, Trp, Tyr) are involved in π-π interactions. Database mining of the Cambridge Structural Database (CSD) and the PDB has increasingly been applied to identify and characterize weak intermolecular interactions in chemical and biological systems. Similarly, Goyal et al. performed a search on several protein structures containing urea or urea derivatives in the PDB. Out of 420 such structures, 61 with urea, and 359 with urea derivatives were bound to proteins. Among these structures, 38% with urea and 25% with urea derivatives were found to form stacking arrangement with the aromatic residues.

Urea-assisted RNA unfolding

Examination of the solute-cosolvent interactions helps us to elucidate the molecular basis behind the RNA unfolding mechanism. Several factors, such as nature of cosolvent, functional groups of nucleic acid structures, sequence dependent effects and other factors contribute to this process. Experimental and theoretical studies have been done to understand the RNA unfolding mechanism in aqueous urea solution. It is interesting to see how RNA molecules scan large number of conformations to reach the desired native state and how denaturant like urea drives the native state towards the unstable unfolded state. Different types of RNA structures such as hairpin loops, tRNAs, riboswitches, RNA pseudoknots, G-quadruplexes, and siRNAs have been

used as models to explore the urea-mediated RNA unfolding mechanism (Timchenko et al. 1993; Holland and Hoffman 1996; Gluick and Yadav 2003; Mahen et al. 2005; Ma et al. 2006; Lambert and Draper 2007; Pincus et al. 2008; Aslanyan et al. 2017). Denaturant effects of urea on the structure, stability, dynamic, and kinetic properties of RNA have been assessed by various experimental techniques like dynamic light scattering, UV absorption spectroscopy, circular dichroism studies, and isothermal urea titration (Timchenko et al. 1993; Shelton et al. 1999; Sosnick 2001; Lambert and Draper 2012). Moreover, effects of osmolytes on the conformational dynamics of DNA hairpin and other nucleic acid functional groups using various techniques like vapor pressure osmometry, fluorescence correlation spectroscopy, and SDS-PAGE studies have shown the utility of urea as a quantitative probe to unravel the nucleic acid denaturation mechanism (Zhang et al. 1996; Bonnet et al. 1998; Griko et al. 2001; Lambert et al. 2010). DNA melting in different osmolytes was quantified by the local-bulk partitioning model earlier (Hong et al. 2004; Nordstrom et al. 2006). Intramolecular Watson-Crick and Hoogsteen hydrogen bonding, base stacking interactions, and hydrophobic bonding provide a basis for structural stability of RNA/DNA molecules. Urea is known to destabilize the native conformations of RNA and to denature the DNA molecules by disrupting the intramolecular hydrogen bonding interactions or by weakening the intermolecular interactions. Few of the experimental and computational studies have been discussed in the following sections.

One major interest is how interactions between different regions of nucleic acids and urea contribute to the stabilization of the unfolded states of RNA. The quest to answer this challenging riddle has led to a number of experimental and theoretical studies to understand the unfolding mechanism. Earlier studies reported that urea induces changes in nucleic acid structures by forming favorable interactions with exposed surfaces of nucleobases compared with other regions, such as backbone, ribose, and phosphate groups (Hong et al. 2004; Lambert and Draper 2012; Guinn et al. 2013; Yoon et al. 2013; Kasavajhala et al. 2015; Miner and García 2017; Alodia et al. 2018; Jaganade et al. 2019). These strong urea nucleobase interactions are quantified by various experimental and theoretical approaches (Gao et al. 2017; Patra et al. 2017; Miner and García 2017). Guinn et al. showed relatively favorable interactions of urea compared with water with different regions of nucleic acids structures, like, heterocyclic aromatic ring, methyl, carbonyl and phosphate O, amino N, and sugar (C and O) (Guinn et al. 2013). Urea has long been used as an analytical tool to characterize the ubiquitous thermodynamic forces stabilizing biomolecular structures. Recent FRET studies indicated an increase in enthalpy and entropy of the RNA/DNA hairpins in the presence of high concentration of urea (Holmstrom and Nesbitt 2014; Holmstrom et al. 2015; Patra et al. 2017). A rugged folding free energy surface of DNA was observed which involves a number of quasi-open intermediate conformations (Sarkar et al. 2009). In high urea concentration, a loss of hydrogen bonding and weakening of base stacking interactions indicate transition of native folded state towards unfolded state. A number of theoretical and experimental studies are available to estimate the unfolding free energy (*m*-value) which is directly proportional to the solvent accessible surface area (Ma et al. 2006; Lambert et al. 2010). Several research groups monitored structural deviations in urea-assisted RNA unfolding transitions using *m*-values which can be correlated with the free energy values obtained from melting temperature studies (Lambert and Draper 2012; Guinn et al. 2013; Moeser and Horinek 2013). It is assumed that total free energy contributing to the urea-biomolecule interactions can be obtained from individual components of biomolecules exposed to solvent surface in native folded and unfolded states. In higher urea concentration, folding rate constant decreases, while significant increase in unfolding rate constant was observed which makes urea a potent denaturant (Sosnick 2001; Auton and Bolen 2005; Lambert and Draper 2007, 2012).

MD simulations have been employed to unravel the urea-RNA unfolding mechanism at the molecular level. For example, Priyakumar et al. showed stable urea nucleobase stacking and hydrogen bonding (see Fig. 5) interactions using RNA hairpin (Priyakumar et al. 2009). Later, Yoon et al. proposed water-induced disruption of RNA followed by

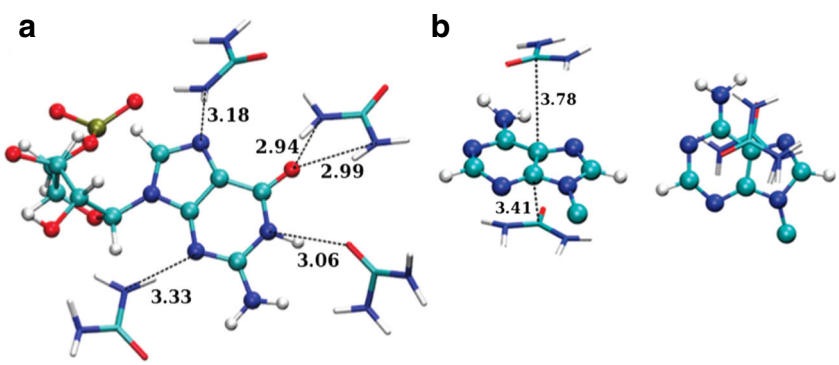

Fig. 5 Interactions involving the RNA hairpin: **a** Hydrogen bonding between urea and RNA base. **b** Stacking between urea and RNA base. Adapted with permission from Priyakumar et al. (2009). Copyright (2009) American Chemical Society

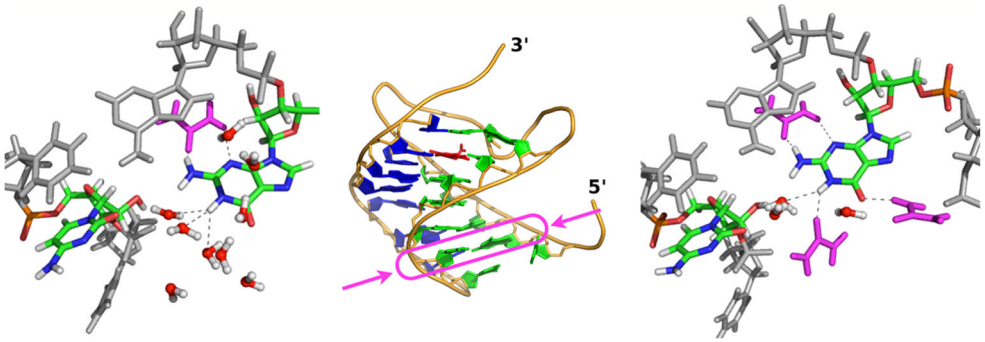

Fig. 6 Urea assisted RNA unfolding: Urea forms favorable interactions with exposed nucleobases in unfolded RNA. The mechanism: water-induced disruption of base pairs (left) resulting in the formation of a "wet" destabilized RNA followed by solvation by urea (right). The structure of preQ1-riboswitch (middle). Reprinted with permission from Yoon et al. (2013). Copyright (2013) American Chemical Society

urea solvation using the PreQ1-riboswitch as a model system (Fig. 6) (Yoon et al. 2013). Furthermore, Garcia et al. studied preferential interactions of RNA with urea and determined the free energy landscape of RNA hairpin using unbiased replica exchange molecular dynamics (REMD) simulations (Miner and García 2017). Recently, the preferential binding of urea to the single-stranded DNA structure was quantified using molecular dynamic simulations, and DNA unfolding is studied using Kirkwood-Buff integrals and transfer free energies and employing metadynamics simulations (Oprzeska-Zingrebe et al. 2019; Oprzeska-Zingrebe and Smiatek 2018). Several quantum mechanical studies revealed that urea indeed forms strong stacking interactions with nucleobases dominated by dispersion (Kasavajhala et al. 2015). The ability of urea to form strong $\pi-$stacking interactions with nucleobases is intriguing. A recent extensive QM calculation investigated the importance of functional groups on nucleobases and studied the effect of urea orientations of the urea-nucleobase stacking interactions (Alodia et al. 2018). Noncovalent stacking interactions were found to be the driving forces, and energetically, these interactions are dominated by dispersion effects.

Preferential interactions of urea with the exposed aromatic surfaces of nucleic acids have been the subject of several experimental and computational studies. Preferential interactions of urea were quantified in several computational studies using a two-domain model and Kirkwood-Buff integrals (Hong et al. 2004; Miner and García 2017; Oprzeska-Zingrebe et al. 2019; Oprzeska-Zingrebe and Smiatek 2018; Jaganade et al. 2019). The mechanism by which urea mediates the protein unfolding is quite different from how urea drives the RNA unfolding and DNA denaturation (Thirumalai and Woodson 1996; Thirumalai and Hyeon 2005). However, it was also analyzed before that polar amide–like accessible surface area of DNA nucleobases and urea interactions showed a similar nature as the polar amide peptide surface and urea interactions (Hong et al. 2004). Urea interacts with nucleobases via different modes of interactions. Figure 7 shows the spatial density distributions of C, N, and O atoms of urea around the nucleobase model system. The nitrogen atom of urea forms NH$-\pi$ stacking and hydrogen bonds with the nucleobase (Yoon et al. 2013; Priyakumar et al. 2009). Oxygen atoms can similarly form hydrogen bonds with donor atoms of the solute molecule. Prominent black regions of carbon atoms above and below the base molecule plane indicate possible NH$-\pi$ and $\pi-\pi$ stacking interactions. Along with the noncovalent driving forces explained in the previous sections, such as stacking, hydrogen bonding and dispersion interactions, enthalpy and internal energy, and entropy of the system are quintessential in understanding the free energy of unfolding in the urea-induced RNA unfolding mechanism. All these observations emphasize the importance of urea-aromatic interactions in the urea-assisted RNA unfolding mechanism.

Urea lesion interaction within damaged DNA

Various factors such as ionizing radiations, chemical reagents, and oxidative stress lead to damage in DNA. DNA damage affects the viability of cell and its fitness and can

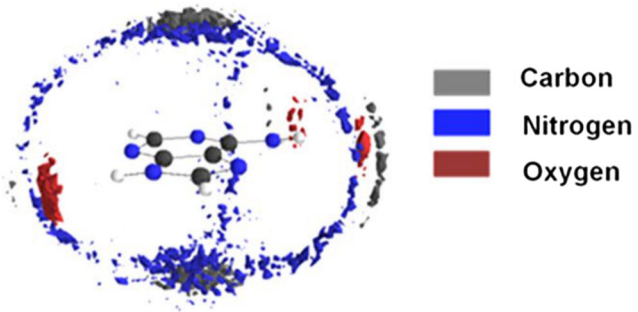

Fig. 7 Most probable positions of urea atoms around the nucleobase model. Adapted with permission from Jaganade et al. (2019). Copyright (2019) Springer Nature

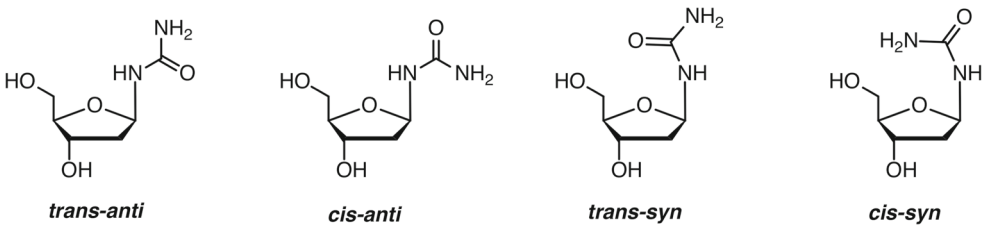

Fig. 8 *syn* and *anti* orientations of urea around the glycosidic bond

lead to uncontrolled growth or cellular death. Though urea has achieved wide attention as a denaturant of proteins and RNA, it is also known as an effective replicative block to the polymerase (Ide et al. 1985). Fragmentation products of different lesions lead to the formation of urea moiety. There are several experimental studies available that provide the basis of the formation of urea lesion. Mutagenic and repair properties have been investigated by incorporating deoxyribosylurea nucleotide into DNA fragments by chromatography experiments (Guy et al. 1990; Baillet and Behr 1995). Ionizing radiation, oxidation of thymine, and degradation of thymine hydroperoxides result in urea formation. 7,8-Dihydro-8-oxoguanine (8-oxoG) is one of the most studied mutagenic lesions which react with oxidative products to give rise to urea lesion. Henderson et al. studied the hydrolysis of oxalauric acid to urea lesion simulated under physiologically relevant conditions (Henderson et al. 2005). It is known that one of the most common damaging agents, thymine glycol undergoes alkali hydrolysis to form urea residues (McNulty et al. 1998). Urea is known to block the replication by DNA polymerase and it is recognized by various repair enzymes, such as N glycosidase, endonuclease III, and exonuclease III. The urea lesion is first recognized by DNA glycosylase, endonuclease III, or endonuclease VIII and later on excised by base excision repair mechanism (Wallace 1994). Moreover, the presence of urea lesion was found to affect the cleavage rates of DNA-RNA hybrids by ribonuclease H. Several experimental studies suggested that the presence of thymine glycol and urea residues interferes with the DNA polymerase activity. Few NMR studies reported structures of urea lesion incorporated in B-DNA duplexes and other few studies explained the role of urea lesion in frameshift mutations (Gervais et al. 1998; Maufrais et al. 2003). Studies have shown that the introduction of urea lesion into the DNA strand gave rise to transition mutations at the urea site (Evans et al. 1993). All these experimental observations are supported by few computational MD studies to understand the dynamic properties of urea-incorporated DNAs. Thermodynamic stability and hydrogen bonding ability of urea have been assessed by free energy calculations and MD simulation (Gervais et al. 1998; Suresh et al. 2016). It is interesting to understand the atomistic details of how urea incorporated DNA maintains its structural integrity.

Urea has sufficient donor and acceptor groups to be involved in hydrogen bonding and it was observed that it forms stable intra- and inter-strand hydrogen bonding and base stacking interactions with bases on the opposite strand of the DNA (Gervais et al. 1998). The carbonyl group of urea, nitrogen atom of the amino group, and oxygen atom can take part in hydrogen bonding formation. It was observed that two isomers of urea in *cis* and *trans* forms showed different structural orientations in helical DNA and that may be due to the difference in hydrogen bonding patterns (Gervais et al. 1992). Moreover, urea is present in *syn* and *anti* orientations around the glycosidic bond with equal probability of occurrence. The *trans-anti* isomer of urea can form hydrogen bonding with the opposite base in intrahelical conformation, while *cis* urea isomer is present in extruded form from the helical axis of the DNA. Figure 8 shows the possible ways in which urea is oriented around the glycosidic bond in the DNA double helix. The urea lesion occupies either extrahelical or intrahelical positions on the DNA helices. Urea-thymine can form regular two hydrogen bonds similar to AT base pair. As mentioned in the earlier sections in this review, various experimental and computational studies revealed that urea can form a stable hydrogen bonding and favorable stacking interactions with the nucleobases in their extrahelical conformations. Recently, Suresh et al. tried to unravel the ability of urea to mimic nucleobases within the nucleic acid structures using MD simulations. Urea was found to form direct hydrogen bonding with purine bases while water-mediated hydrogen bonding was observed in urea-pyrimidine base interactions (Suresh et al. 2016). In Fig. 9, the two modes of interaction of urea with nucleobases are shown. The ability of urea to take part in favorable stacking with nucleobases was suggested to assist in retaining the intrahelical conformation of urea even when it is not involved in direct hydrogen bonding interactions with the pyrimidine base.

Urea conduction through membrane proteins

Proteins mediating the permeation of ions and small molecules across cellular membranes are typically known as membrane transport proteins. Membrane channels

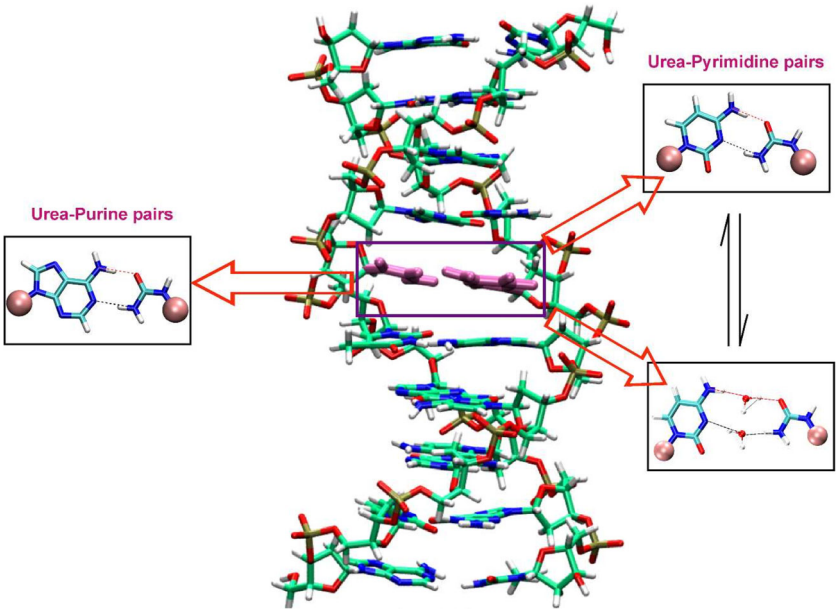

Fig. 9 Modes of the interaction of urea with pyrimidine and purine bases when it is intercalated in the DNA double helix. Reprinted with permission from Suresh et al. (2016). Copyright (2016) American Chemical Society

responsible for selective exchange of water-soluble materials, e.g., water, ions, and other nutrients, across cell membranes are abundant in all forms of life, including mammals, amphibians, insects, plants, and bacteria (Gonen et al. 2004; Mathai et al. 1996; Levin et al. 2012; Deng et al. 2015; Lucien et al. 2002; Wang and Tajkhorshid 2007; Bai et al. 2017; Esteva-Font et al. 2015; Weeks et al. 2004; Hunger et al. 2014; Abreu et al. 2010; Padhi et al. 2013, 2017; Ramakrishnaet al. 2015; Padhi and Priyakumar 2017, 2020). Unlike water-soluble proteins, hydrophobic residues of membrane proteins are exposed towards the membrane instead of being buried in the protein interior. Conversely, hydrophilic residues can reside on the protein surface, outside the membrane, neighboring the lipid headgroups, even sometimes, in the protein interior, for example, while forming a channel (Harris and Booth 2012; Ramakrishna et al. 2015; Padhi et al. 2015). Recent advances in experimental structural biology and computer simulation methodologies have facilitated our understanding on the structural and functional bases of membrane channels at atomic resolution. This section discusses urea transporters (UT)—channel-like proteins, which selectively allow the permeation of urea molecules across a lipid bilayer of the cell—and looks at emerging evidence from experiments and simulations of the urea permeation mechanism how selectivity urea binds to certain amino acid residues to modulate the permeation process.

Experimental signatures: Urea transporters play an important role in urea excretion and maintaining water balance for a variety of living organisms. UT members have been found in various species including bacteria, fungi, insects, and vertebrates including all mammals. The mammalian urea transporters are of two forms: UT-A (with 6 isoforms) and UT-B (with 2 isoforms) (Sands 2003; Smith 2009). These UTs have many homologues in bacteria, such as ApUT (*Actinobacillus pleuropneumoniae* urea transporter) (Godara et al. 2009) which was later used for urea permeation study (Raunser et al. 2009). The field of urea transport has a long history (Hediger et al. 1996; Gamble et al. 1934; Aukland 1961; Gallucci et al. 1971; Macey 1984; Mayrand and Levitt 1983; Sands and Knepper 1987; Schafer et al. 1974; Kishore et al. 1997; Smith and Rousselet 2001; Zhao et al. 2007). However, the atomic resolution structure of UT was not resolved until 2009. The first crystal structure of a UT family member was the bacterial protein dvUT (Levin et al. 2009), a functional homologue of mammalian UTs from *Desulfovibrio vulgaris* (PDB IDs: 3K3F and 3K3G of dvUT alone and co-crystallized with the urea analogue dimethylurea, respectively). The same group subsequently resolved the X-ray crystal structure of the mammalian UT-B from *Bos taurus* (Levin et al. 2012) (PDB IDs: 4EZC and 4EZD of UT-B alone and co-crystallized with the urea analogue selenourea, respectively). X-ray crystallography revealed a low-pH structure of the proton-gated urea channel from *Helicobacter pylori*, HpUreI (Strugatsky et al. 2013), at a resolution of 3.3 Å (PDB ID: 3UX4). Later, the cryo-electron microscopy (cryo-EM) structures of the same in close and open conformations were solved both at a resolution of 2.7 Å (Cui et al. 2019). These three-dimensional atomic-resolution structures have served as invaluable tools for us to understand the functional characteristics of UTs. Particularly, dvUT and UT-B are homologous. Both of them are trimers, and each monomer can diffuse urea

or urea analogues, individually. It is therefore, likely that the basic nature of the core hydrophobic regions of the UT family, including the ten transmembrane-helix topology as well as the location of the permeation pathway follow a conserved signature motif across the UT family (Levin and Zhou 2014). It is intriguing that all known structures have aromatic amino acid residues lining the selectivity filter (Fig. 10).

Atomistic simulations: An atomistic understanding of the three-dimensional structures of membrane transport proteins is essential to determine the mechanistic details of the functional properties, such as conduction and selectivity. Advanced computational protocols are now increasingly becoming complementary tools to study such atomistic details though biological membranes are complex in terms of their molecular compositions, structures, and functions over a wide range of time scales, and characterized by nonequilibrium conditions (Pieńko and Trylska 2019; Enkavi et al. 2019; Na et al. 2018). An umbrella sampling MD simulation study was performed on first X-ray crystal structure of UT-B in a pioneering work by Levin et al. (2012). Here they showed that the selectivity filter has two urea binding sites. The associated potential of mean force (PMF) located two almost symmetric pairs of energy minima in the S_o and S_i regions with an energy barrier as large as approximately 5.0 kcal mol^{-1}. Wang et al. studied both urea and water transport through the dvUT using MD simulations, Monte Carlo methods, and the adaptive biasing force approach (Wang et al. 2015b). A computational study modeled the urea flux in dvUT, the equilibrium urea binding to dvUT, as well as the substitution of urea by DMU in the dvUT (Zhang et al. 2017). Another investigation by Padhi and co-workers elucidated the urea permeation mechanism employing umbrella sampling MD simulations (Padhi and Priyakumar 2016). They proposed that urea-aromatic interactions arising from parallelly arranged aromatic rings in the pore lowers the energy barrier for urea transport. This stacking type interaction between urea and four phenylalanine side chains is similar to that discussed in the previous sections. For the first time, a multiple urea transport model was proposed here. An alternative approach, unbiased equilibrium microsecond long MD simulations, was used to study the urea conduction in HpUreI at atomic detail (McNulty et al. 2013). This simulation identified that two consecutive constrictions open to allow conduction of urea which interacts with highly conserved residues those determine selectivity and, in turn control urea flux through the channel. In fact, they showed that HpUreI conducts water at rates almost equivalent to aquaporins which is a family of membrane channel responsible for permeation of water (Wang and Tajkhorshid 2007; Dynowski et al. 2008).

Urea has a stronger dipole moment (4.6 D) than water (1.8 D), resulting in low solubility in lipids. It shows slow permeability across lipid bilayers those lack any transport proteins to facilitate the diffusion (Finkelstein 1976). Despite having such high polarity, urea readily permeates through the UT channel whose hydrophobic constriction region is lined by aromatic residues. Residues lining the selectivity filters of dvUT, bovine UT-B, and HpUreI pores are depicted in Fig. 10a, b, and c, respectively. The HpUreI crystal structure revealed two constrictions, periplasmic, C_P and cytoplasmic, C_C in the channel. The key aromatic residues were found to be Phe84 and Trp149 for the C_P, and Tyr88 and Trp153 for the C_C. During the transport through C_P, urea was found to be interacting with the aromatic Phe84 on one side, and on the other side, with the Trp149 while indole donating a hydrogen bond to urea. When urea traverses through C_C, on one side, it remains in close contact with the Trp153, and on the other side with the Tyr88, whose phenol is in hydrogen bonding interactions with urea (see Fig. 10c). Currently, there are no crystal structures available for any known UT protein bound to urea, except the dvUT bound to DMU (Levin et al. 2009) and bovine UT-B bound to selenourea (Levin et al. 2012).

Although both bacterial dvUT and mammalian UT-B proteins hold an entirely different channel-architecture compared with HpUreI, remarkable similarities were observed in the prominent arrangement of combinations of aromatic and other hydrophobic residues in the pore-lining (Levin et al. 2009). For both channel types, a urea molecule has to transport through the pore sandwiched between either a pair of aromatic residues or an aromatic and a hydrophobic residues, while the latter is involved in hydrogen bonding as illustrated in Fig. 10c (Strugatsky et al. 2013; Levin et al. 2012). This may ensure high selectivity for a planar molecule like urea that is also highly polar. Their results indicate that the interaction of urea with aromatic rings, which may involve both amide-π stacking (Imai et al. 2009) and hydrogen bonding, likely to play crucial roles in the urea permeation. Similarly, in a recent computational study on dvUT, phenylalanine ring pairs (Phe190/Phe243 and Phe80/Phe27) were found to be the key residues which involved in stacking interactions with urea molecules inside the pore (Padhi and Priyakumar 2016).

Protein-ligand interactions

Noncovalent interactions, in particular aromatic stacking interactions, are essential in chemistry and biology to

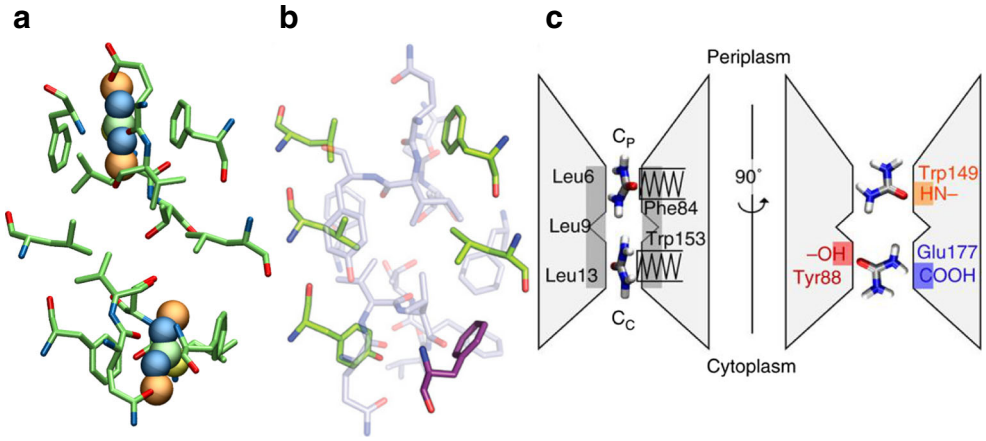

Fig. 10 Residues lining the selectivity filter of the **a** dvUT-dimethylurea complex (PDB ID: 3k3g) (Levin et al. 2009) and the **b** bovine UT-B. Adapted with permission from Levin et al. (2012). Copyright (2012) National Academy Sciences. **c** HpUreI: In a schematic view, urea is sandwiched between conserved residues, while making hydrogen bonds with orthogonally oriented side chains. Adapted with permission from McNulty et al. (2013). Copyright (2013) Springer Nature

understand the correct description of the structure and properties of molecules (Meyer et al. 2003; Schottel et al. 2008; Waters 2002; Riley and Hobza 2012; Wheeler 2012; Daze and Hof 2012; Macias et al. 2003; Ma and Dougherty 1997; Dougherty 2012; Tsuzuki et al. 2000a, b; Müller-Dethlefs and Hobza 2000). The growing experimental as well as in silico approaches specifically studies of small aromatic model systems (Bissantz et al. 2010; Meyer et al. 2003; Jarvis and Ouvry 2019; Wang et al. 2015a; Bootsma and Wheeler 2018; Toupkanloo and Rahmani 2018; Alodia et al. 2018; Jaganade et al. 2019; Goyal et al. 2017; Casals-Sainz et al. 2019) have been providing significant insight into the relative contribution of energetical and geometrical preference of different stacking partners, for example, $\pi-\pi$ (Burley and Petsko 1985; Riley and Hobza 2012; Riley et al. 2010; Su et al. 2014; Scrutton and Raine 1996; Su and Li 2009; Jeziorski et al. 1994), anion$-\pi$ (Schug and Lindner 2005; Schottel et al. 2008), cation$-\pi$ (Dougherty 2012; Salonen et al. 2009; Scrutton and Raine 1996), and XH$-\pi$ (Tsuzuki et al. 2000a, b). This knowledge is routinely used in structure-based drug design and molecular recognition.

Amide-aromatic stacking interactions

A significant part of the π-interactions in proteins focuses on the aromatic side chains. In 2013, Harder et al. revealed a noncanonical intermolecular interaction where, the $\pi-$system of an amide is engaged in stacking arrangement with arenes (Harder et al. 2013). The Diederich lab has been so far taken the lead in increasing our understanding of these interactions and the knowledge gained from this structure-activity relationship study and the detection of the binding mode has been continuing to inspire their use in rational design (Giroud et al. 2016; Salonen et al. 2009; Salonen et al. 2011; Salonen et al. 2012; Lauber et al. 2016; Ehmke et al. 2013; De Gasparo et al. 2018). These relatively less explored amide stacking interactions are energetically stronger than other stacking interactions, and can be competitive with hydrogen bonds (James et al. 2009, 2011); they can also play a significant role in protein structure and stability (Kemmink et al. 1993; Duan et al. 2000a, b), and similar interactions have been suggested in urea-induced denaturation of proteins (Goyal et al. 2017).

Systematic analyses of the PDB protein-ligand complexes detected amide-arene stacking interactions between protein backbone and π surfaces of ligands as one of the relatively frequent interactions (Harder et al. 2013; Giroud et al. 2016; Giroud et al. 2017; de Freitas and Schapira 2017). In a series of studies of small-molecule inhibitors, amide stacking interactions have been found to modulate selectivity towards the target. For instance, Roehrig et al. observed that introduction of an amide into an oxazolidinone-based inhibitor increased the binding affinity in case of serine protease Factor Xa (FXa) (Roehrig et al. 2005). Here, the morpholinone moiety was found to be sandwiched between Tyr and Phe (see Fig. 11a). Whereas, Diederich et al. (Salonen et al. 2012) optimized the relative orientation of the oxazole linker in a small-molecule inhibitor, w.r.t. the amide backbone in the binding pocket that improved the binding affinity. A co-crystal structure of triazine nitrile binding to human cathepsin L (hCatL) (Ehmke et al. 2013) revealed chlorobenzyl ring of triazine nitrile ligand stacks on the Gly67–Gly68 peptide bond (Fig. 11b). Many other studies have delineated the impor-

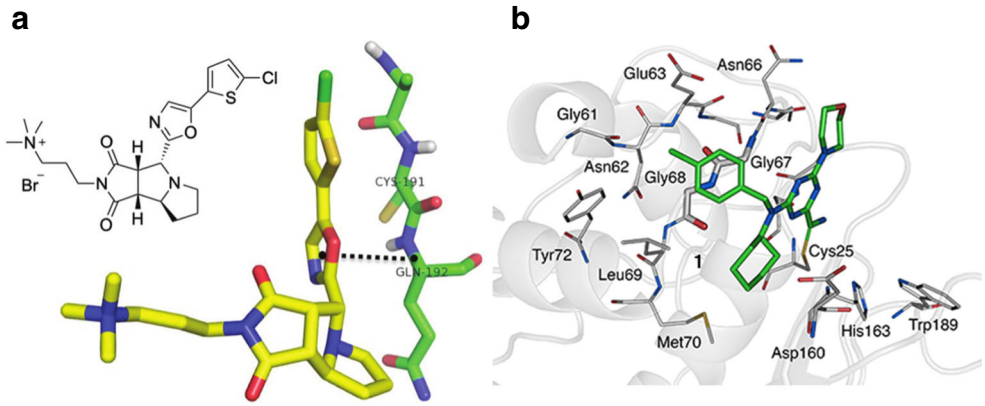

Fig. 11 **a** Factor Xa inhibitor (left), and it is interacting with Gln192 in the complexed crystal structure (PDB ID: 2Y5G). Reprinted with permission from DeFrees et al. (2019). Copyright (2019) Royal Society of Chemistry. **b** Co-crystal structure of triazine nitrile with human cathepsin L (hCatL) (PDB ID: 4AXM, resolution 2.80 Å). The chlorobenzyl ring of the ligand stacks on the Gly67–Gly68 peptide fragment. Adapted with permission from Giroud et al. (2016). Copyright (2016) John Wiley and Sons

tance of heteroarene-amide interactions for ligand binding including FXa (Parrish et al. 2017; Shi et al. 2008) and bacterial serine hydrolase CTX-M (DeFrees et al. 2019). Optimizing amide stacking as well exhibited improved binding affinity to targets, including the aspartic protease endothiapepsin (Hartman et al. 2015), protein kinase A (PKA) (Lauber et al. 2016), cysteine protease rhodesain (Ehmke et al. 2013), and the cysteine protease autophagin-1 (Qiu et al. 2016).

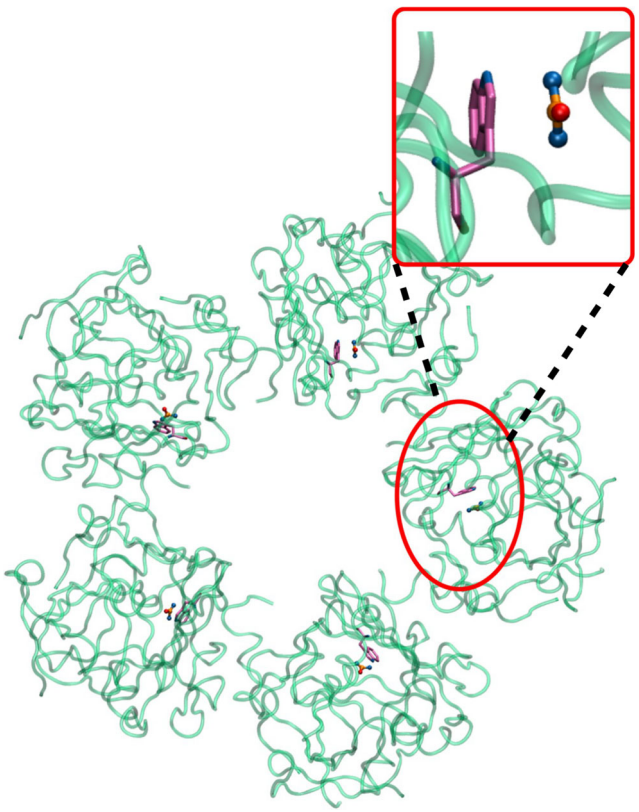

Fig. 12 Co-crystal structure of urea with YedY (consisting of 5 monomers) from *Escherichia coli*, highlighting the arrangement of the tryptophan residue interacting with a urea molecule via stacking. (PDB ID: 1XDQ, ref. (Loschi et al. 2004))

Similar to protein backbone amide moiety, urea too is an amide. Consequently, urea-aromatic interactions might prove to be a significant contributing factor in drug design as seen for amide-aromatic interactions. In fact, in an earlier investigation (Loschi et al. 2004), urea was found to bind to the active site in YedY structure (PDB ID: 1XDQ, Fig. 12), suggesting a viable role of urea as a weak substrate analogue inhibitor. A series of crystal structures of YEATS-domain containing protein MLLT1 (ENL) complexed with piperazine-urea derivatives have been deposited in the PDB (IDs: 6T1I, 6T1J, and 6T1L) very recently (Ni et al. 2019). In all these three structures, Tyr is interacting with the O=C–N moiety of the urea derivative in a stacked arrangement (see Fig. 13). Small-molecule screening has identified potent and selective inhibitors for various UTs. Additionally, emerging evidence from experiments suggests that UT inhibitors can be developed as a novel class of diuretic drugs (Esteva-Font et al. 2015; Yao et al. 2012; Zhao et al. 2019; Lee et al. 2018; Li et al. 2014; Li et al. 2019). Understanding the mechanism of binding and permeation of urea and urea analogues across UTs might be useful structural determinants which may aid in optimizing the binding of clinically useful UT inhibitors. High-affinity urea-binding sites would be promising contacts for future study. Mining of large crystallographic data sets would uncover the urea/urea derivative involved in aromatic interactions in protein structure and also in protein-ligand binding. Exploring the conformational space of small-molecule ligands, and their target-bound state will lead to a better understanding of the forces that guide molecular recognition. Optimizing these interactions can provide a potential route to enhanced drug binding.

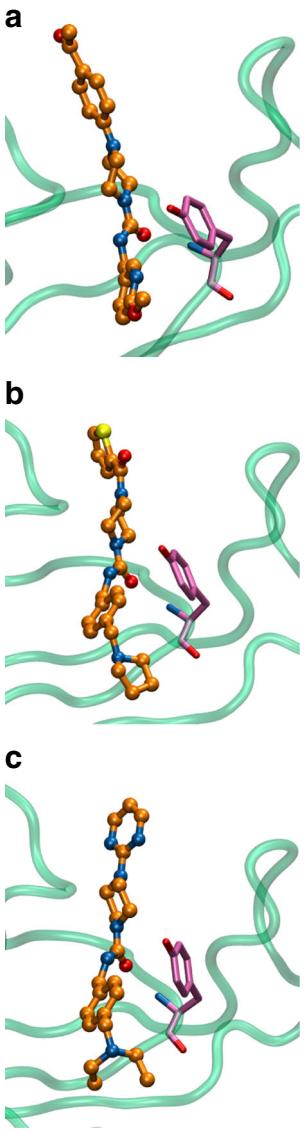

Fig. 13 Co-crystal structures of three piperazine-urea derivatives with YEATS-domain containing protein MLLT1 (ENL) (Ni et al. 2019) (PDB IDs: 6T1I, 6T1J and 6T1L). Tyrosine residue is in stacking arrangement with the O=C–N group of the urea derivative in all three structures (**a**), (**b**), and (**c**)

Summary

Both experimental and computational studies have played major roles in understanding the mechanism of urea-assisted protein unfolding. While dispersion interactions are suggested to be largely responsible for stabilizing unfolded protein conformations in aqueous urea, the nature of these interactions is still under study. Detailed computational exercises were crucial in identifying the stacking interaction between urea and aromatic groups in proteins/RNA to be a contributing factor. The aromatic groups are capable of forming NH-π and hydrogen bonding interactions, but similar interactions are possible with water as well and hence stacking is found to be primarily responsible for stabilizing the solvent exposed aromatic groups of proteins and nucleic acids in the presence of urea. Such stacking interactions are also found to be a major contributor for maintaining the helical integrity of damaged DNA with urea lesions. All the three urea transporter structures that have been solved so far have aromatic residues lining the selectivity filter of the pore in the protein. Detailed molecular dynamics simulations indicate a urea-aromatic stacking enabled mechanism of regulating urea permeation in this class of proteins. Survey of crystal structures clearly demonstrate the prevalence of urea-aromatic stacking between urea derivatives and aromatic residues. Such an overwhelming presence of novel and non-intuitive nonbonding interaction involving urea and aromatic groups encourages further applications in drug design. While urea is capable of forming hydrophobic/dispersion type interactions with aromatic groups perpendicular to the molecular plane, the presence of polar O/N atoms in the molecule inherently supports in-plane hydrogen bond interactions. Further investigations on how to leverage such a dual role of urea would be valuable in drug design projects.

Funding information We thank the DST-SERB (grant nos. EMR/2016/007697 and grant no. PDF/2018/000142) for financial support.

References

Abreu C, Sanguinetti M, Amillis S, Ramon A (2010) Urea, the major urea/H+ symporter in aspergillus nidulans. Fungal Genet Biol 47(12):1023–1033

Alodia N, Jaganade T, Priyakumar UD (2018) Quantum mechanical investigation of the nature of nucleobase-urea stacking interaction, a crucial driving force in RNA unfolding in aqueous urea. J Chem Sci 130(11):158

Aslanyan L, Ko J, Kim BG, Vardanyan I, Dalyan YB, Chalikian TV (2017) Effect of urea on G-quadruplex stability. J Phys Chem B 121(27):6511–6519

Aukland K (1961) Renal tubular permeability to urea with special reference to accumulation of urea in the renal medulla. Scand J Clin Lab Invest 13(4):646–660

Aune KC, Tanford C (1969) Thermodynamics of the denaturation of lysozyme by guanidine hydrochloride. ii. dependence on denaturant concentration at 25. Biochem 8(11):4586–4590

Auton M, Bolen DW (2004) Additive transfer free energies of the peptide backbone unit that are independent of the model compound and the choice of concentration scale. Biochem 43(5):1329–1342

Auton M, Bolen DW (2005) Predicting the energetics of osmolyte-induced protein folding/unfolding. Proc Natl Acad Sci USA 102(42):15065–15068

Auton M, Holthauzen LMF, Bolen DW (2007) Anatomy of energetic changes accompanying urea-induced protein denaturation. Proc Natl Acad Sci USA 104(39):15317–15322

Auton M, Bolen DW, Rösgen J (2008) Structural thermodynamics of protein preferential solvation: osmolyte solvation of proteins, aminoacids, and peptides. Proteins: Struct Funct Bioinf 73(4):802–813

Bai X, Moraes TF, Reithmeier RA (2017) Structural biology of solute carrier (slc) membrane transport proteins. Mol Membr Biol 34(1-2):1–32

Baillet S, Behr JP (1995) Deoxyribosylurea and deoxyribosylformamide oligonucleotides. Tetrahedron lett 36(49):8981–8984

Bandyopadhyay D, Mohan S, Ghosh SK, Choudhury N (2014) Molecular dynamics simulation of aqueous urea solution: is urea a structure breaker? J Phys Chem B 118(40):11757–11768

Bellissent-Funel MC, Hassanali A, Havenith M, Henchman R, Pohl P, Sterpone F, van der Spoel D, Xu Y, García AE (2016) Water determines the structure and dynamics of proteins. Chem Rev 116(13):7673–7697

Bennion BJ, Daggett V (2003) The molecular basis for the chemical denaturation of proteins by urea. Proc Natl Acad Sci USA 100(9):5142–5147

Bissantz C, Kuhn B, Stahl M (2010) A medicinal chemist's guide to molecular interactions. J Med Chem 53(14):5061–5084

Bolen DW, Rose GD (2008) Structure and energetics of the hydrogen-bonded backbone in protein folding. Annu Rev Biochem 77:339–362

Bonnet G, Krichevsky O, Libchaber A (1998) Kinetics of conformational fluctuations in DNA hairpin-loops. Proc Natl Acad Sci USA 95(15):8602–8606

Bootsma AN, Wheeler SE (2018) Stacking interactions of heterocyclic drug fragments with protein amide backbones. ChemMedChem 13(8):835–841

Burley S, Petsko GA (1985) Aromatic-aromatic interaction: a mechanism of protein structure stabilization. Science 229(4708):23–28

Canchi DR, García AE (2011) Backbone and side-chain contributions in protein denaturation by urea. Biophys J 100(6):1526–1533

Canchi DR, García AE (2013) Cosolvent effects on protein stability. Annu Rev Phys Chem 64:273–293

Canchi DR, Paschek D, García AE (2010) Equilibrium study of protein denaturation by urea. J Am Chem Soc 132(7):2338–2344

Casals-Sainz JL, Castro AC, Francisco E, Pendás ÁM (2019) Tetrel interactions from an interacting quantum atoms perspective. Molecules 24(12):2204

Cheng X, Shkel IA, O'Connor K, Henrich J, Molzahn C, Lambert D, Record Jr MT (2017) Experimental atom-by-atom dissection of amide–amide and amide–hydrocarbon interactions in H2O. J Am Chem Soc 139(29):9885–9894

Chitra R, Smith PE (2000) Molecular dynamics simulations of the properties of cosolvent solutions. J Phys Chem B 104(24):5854–5864

Cui Y, Zhou K, Strugatsky D, Wen Y, Sachs G, Zhou ZH, Munson K (2019) ph-dependent gating mechanism of the helicobacter pylori urea channel revealed by cryo-em. Sci Adv 5(3):eaav8423

Daze KD, Hof F (2012) The cation-π interaction at protein–protein interaction interfaces: Developing and learning from synthetic mimics of proteins that bind methylated lysines. Acc Chem Res 46(4):937–945

De Gasparo R, Brodbeck-Persch E, Bryson S, Hentzen NB, Kaiser M, Pai EF, Krauth-Siegel RL, Diederich F (2018) Biological evaluation and X-ray co-crystal structures of cyclohexylpyrrolidine ligands for trypanothione reductase, an enzyme from the redox metabolism of trypanosoma. ChemMedChem 13(9):957–967

DeFrees K, Kemp MT, ElHilali-Pollard X, Zhang X, Mohamed A, Chen Y, Renslo AR (2019) An empirical study of amide–heteroarene π-stacking interactions using reversible inhibitors of a bacterial serine hydrolase. Org Chem Front 6:1749–1756

Delanghe S, Delanghe JR, Speeckaert R, Van Biesen W, Speeckaert MM (2017) Mechanisms and consequences of carbamoylation. Nat Rev Nephrol 13(9):580–593

Deng D, Sun P, Yan C, Ke M, Jiang X, Xiong L, Ren W, Hirata K, Yamamoto M, Fan S et al (2015) Molecular basis of ligand recognition and transport by glucose transporters. Nature 526(7573):391

Dougherty DA (2012) The cation-π interaction. Acc Chem Res 46(4):885–893

Duan G, Smith VH, Weaver DF (2000a) Characterization of aromatic-amide (side-chain) interactions in proteins through systematic ab initio calculations and data mining analyses. J Phys Chem A 104(19):4521–4532

Duan G, Smith VHJr, Weaver DF (2000b) A data mining and ab initio study of the interaction between the aromatic and backbone amide groups in proteins. Int J Quantum Chem 80(1):44–60

Duffy EM, Kowalczyk PJ, Jorgensen WL (1993a) Do denaturants interact with aromatic hydrocarbons in water? J Am Chem Soc 115(20):9271–9275

Duffy EM, Severance DL, Jorgensen WL (1993b) Urea: potential functions, log p, and free energy of hydration. Isr J Chem 33(3):323–330

Dunning TH (1989) Gaussian basis sets for use in correlated molecular calculations. i. the atoms boron through neon and hydrogen. J Chem Phys 90(2):1007–1023

Dynowski M, Mayer M, Moran O, Ludewig U (2008) Molecular determinants of ammonia and urea conductance in plant aquaporin homologs. FEBS Lett 582(16):2458–2462

Ehmke V, Winkler E, Banner DW, Haap W, Schweizer WB, Rottmann M, Kaiser M, Freymond C, Schirmeister T, Diederich F (2013) Optimization of triazine nitriles as rhodesain inhibitors: Structure–activity relationships, bioisosteric imidazopyridine nitriles, and X-ray crystal structure analysis with human cathepsin l. ChemMedChem 8(6):967–975

England JL, Haran G (2011) Role of solvation effects in protein denaturation: from thermodynamics to single molecules and back. Annu Rev Phys Chem 62:257–277

England JL, Pande VS, Haran G (2008) Chemical denaturants inhibit the onset of dewetting. J Am Chem Soc 130(36):11854–11855

Enkavi G, Javanainen M, Kulig W, Róg T, Vattulainen I (2019) Multiscale simulations of biological membranes: the challenge to understand biological phenomena in a living substance. Chem Rev 119(9):5607–5774

Esteva-Font C, Anderson MO, Verkman AS (2015) Urea transporter proteins as targets for small-molecule diuretics. Nat Rev Nephrol 11(2):113

Evans J, Maccabee M, Hatahet Z, Courcelle J, Bockrath R, Ide H, Wallace S (1993) Thymine ring saturation and fragmentation products: lesion bypass, misinsertion and implications for mutagenesis. Mutation Research/Genetic Toxicology 299(3-4):147–156

Finer E, Franks F, Tait M (1972) Nuclear magnetic resonance studies of aqueous urea solutions. J Am Chem Soc 94(13):4424–4429

Finkelstein A (1976) Water and nonelectrolyte permeability of lipid bilayer membranes. J Gen Physiol 68(2):127–135

Finkelstein A, Galzitskaya O (2004) Physics of protein folding. Phys Life Rev 1(1):23–56

Frank HS, Franks F (1968) Structural approach to the solvent power of water for hydrocarbons; urea as a structure breaker. J Chem Phys 48(10):4746–4757

de Freitas RF, Schapira M (2017) A systematic analysis of atomic protein–ligand interactions in the PDB. Med Chem Comm 8(10):1970–1981

Gallucci E, Micelli S, Lippe C (1971) Non-electrolyte permeability across thin lipid membranes. Arch Int Physiol Biochim 79(5):881–887

Gamble J, McKhann C, Butler A, Tuthill E (1934) An economy of water in renal function referable to urea. Am J Physiol 109(1):139–154

Ganguly P, Boserman P, van der Vegt NF, Shea JE (2017) Trimethylamine n-oxide counteracts urea denaturation by inhibiting protein–urea preferential interaction. J Am Chem Soc 140(1):483–492

Gao M, Arns L, Winter R (2017) Modulation of the thermodynamic signatures of an RNA thermometer by osmolytes and salts. Angew Chem Int Ed 56(9):2302–2306

Gervais V, Guy A, Teoule R, Fazakerley G (1992) Solution conformation of an oligonucleotide containing a urea deoxyribose residue in front of a thymine. Nucleic Acids Res 20(24):6455–6460

Gervais V, Cognet JA, Guy A, Cadet J, Téoule R, Fazakerley GV (1998) Solution structure of n-(2-deoxy-D-erythropentofuranosyl) urea frameshifts, one intrahelical and the other extrahelical, by nuclear magnetic resonance and molecular dynamics. Biochemistry 37(4):1083–1093

Giroud M, Harder M, Kuhn B, Haap W, Trapp N, Schweizer WB, Schirmeister T, Diederich F (2016) Fluorine scan of inhibitors of the cysteine protease human cathepsin l: Dipolar and quadrupolar effects in the π-stacking of fluorinated phenyl rings on peptide amide bonds. Chem Med Chem 11(10):1042–1047

Giroud M, Ivkovic J, Martignoni M, Fleuti M, Trapp N, Haap W, Kuglstatter A, Benz J, Kuhn B, Schirmeister T et al (2017) Inhibition of the cysteine protease human cathepsin l by triazine nitriles: Amide...heteroarene π-stacking interactions and chalcogen bonding in the s3 pocket. ChemMedChem 12(3):257–270

Gluick TC, Yadav S (2003) Trimethylamine n-oxide stabilizes RNA tertiary structure and attenuates the denaturating effects of urea. J Am Chem Soc 125(15):4418–4419

Godara G, Smith C, Bosse J, Zeidel M, Mathai J (2009) Functional characterization of actinobacillus pleuropneumoniae urea transport protein, apUT. Am J Physiol Regul Integr Comp Physiol 296(4):R1268–R1273

Gonen T, Sliz P, Kistler J, Cheng Y, Walz T (2004) Aquaporin-0 membrane junctions reveal the structure of a closed water pore. Nature 429(6988):193

Goyal S, Chattopadhyay A, Kasavajhala K, Priyakumar UD (2017) Role of urea–aromatic stacking interactions in stabilizing the aromatic residues of the protein in urea-induced denatured state. J Am Chem Soc 139(42):14931–14946

Granick S, Bae SC (2008) A curious antipathy for water. Science 322(5907):1477–1478

Griko Y, Sreerama N, Osumi-Davis P, Woody RW, Woody AYM (2001) Thermal and urea-induced unfolding in T7 RNA polymerase: calorimetry, circular dichroism and fluorescence study. Protein Science 10(4):845–853

Guinn EJ, Pegram LM, Capp MW, Pollock MN, Record MT (2011) Quantifying why urea is a protein denaturant, whereas glycine betaine is a protein stabilizer. Proc Natl Acad Sci USA 108(41):16932

Guinn EJ, Schwinefus JJ, Cha HK, McDevitt JL, Merker WE, Ritzer R, Muth GW, Engelsgjerd SW, Mangold KE, Thompson PJ et al (2013) Quantifying functional group interactions that determine urea effects on nucleic acid helix formation. J Am Chem Soc 135(15):5828–5838

Guinn EJ, Jagannathan B, Marqusee S (2015) Single-molecule chemomechanical unfolding reveals multiple transition state barriers in a small single-domain protein. Nat Comm 6:6861

Guy A, Ahmad S, Téoule R (1990) Insertion of the fragile 2'-deoxyribosylurea residue into oligodeoxynucleotides. Tetrahedron Lett 31(40):5745–5748

Hall D, Kinjo AR, Goto Y (2018) A new look at an old view of denaturant induced protein unfolding. Anal Biochem 542:40–57

Harder M, Kuhn B, Diederich F (2013) Efficient stacking on protein amide fragments. ChemMedChem 8(3):397–404

Harris NJ, Booth PJ (2012) Folding and stability of membrane transport proteins in vitro. BBA-Biomembranes 1818(4):1055–1066

Hartman A, Mondal M, Radeva N, Klebe G, Hirsch A (2015) Structure-based optimization of inhibitors of the aspartic protease endothiapepsin. Int J Mol Sci 16(8):19184–19194

Hediger MA, Smith CP, You G, Lee WS, Kanai Y, Shayakul C (1996) Structure, regulation and physiological roles of urea transporters. Kidney Int 49(6):1615–1623

Henderson PT, Neeley WL, Delaney JC, Gu F, Niles JC, Hah SS, Tannenbaum SR, Essigmann JM (2005) Urea lesion formation in DNA as a consequence of 7, 8-dihydro-8-oxoguanine oxidation and hydrolysis provides a potent source of point mutations. Chem Res Toxicol 18(1):12–18

Hoccart X, Turrell G (1993) Raman spectroscopic investigation of the dynamics of urea–water complexes. J Chem Phys 99(11):8498–8503

Holehouse AS, Garai K, Lyle N, Vitalis A, Pappu RV (2015) Quantitative assessments of the distinct contributions of polypeptide backbone amides versus side chain groups to chain expansion via chemical denaturation. J Am Chem Soc 137(8):2984–2995

Holland JA, Hoffman DW (1996) Structural features and stability of an RNA triple helix in solution. Nucleic Acids Res 24(14):2841–2848

Holmstrom ED, Nesbitt DJ (2014) Single-molecule fluorescence resonance energy transfer studies of the human telomerase RNA pseudoknot: temperature-/urea-dependent folding kinetics and thermodynamics. J Phys Chem B 118(14):3853–3863

Holmstrom ED, Dupuis NF, Nesbitt DJ (2015) Kinetic and thermodynamic origins of osmolyte-influenced nucleic acid folding. J Phys Chem B 119(9):3687–3696

Hong J, Capp MW, Anderson CF, Saecker RM, Felitsky DJ, Anderson MW, Record MT (2004) Preferential interactions of glycine betaine and of urea with DNA: implications for DNA hydration and for effects of these solutes on DNA stability. Biochem 43(46):14744–14758

Horinek D, Netz RR (2011) Can simulations quantitatively predict peptide transfer free energies to urea solutions? thermodynamic concepts and force field limitations. J Phys Chem A 115(23):6125–6136

Hua L, Zhou R, Thirumalai D, Berne B (2008) Urea denaturation by stronger dispersion interactions with proteins than water implies a 2-stage unfolding. Proc Natl Acad Sci USA 105(44):16928–16933

Hunger D, Doberenz C, Sawers RG (2014) Identification of key residues in the formate channel FocA that control import and export of formate. Biol Chem 395(7-8):813–825

Ide H, Kow YW, Wallace SS (1985) Thymine glycols and urea residues in m13 DNA constitute replicative blocks in vitro. Nucleic Acids Res 13(22):8035–8052

Imai YN, Inoue Y, Nakanishi I, Kitaura K (2009) Amide–π interactions between formamide and benzene. J Comput Chem 30(14):2267–2276

Jaganade T, Chattopadhyay A, Pazhayam NM, Priyakumar UD (2019) Energetic, structural and dynamic properties of nucleobase-urea interactions that aid in urea assisted RNA unfolding. Sci Rep 9(8805):2045–2322

James IIIWH, Müller CW, Buchanan EG, Nix MG, Guo L, Roskop L, Gordon MS, Slipchenko LV, Gellman SH, Zwier TS (2009) Intramolecular amide stacking and its competition with hydrogen bonding in a small foldamer. J Am Chem Soc 131(40):14243–14245

James IIIWH, Buchanan EG, Guo L, Gellman SH, Zwier TS (2011) Competition between amide stacking and intramolecular h bonds

in γ-peptide derivatives: controlling nearest-neighbor preferences. J Phys Chem A 115(43):11960–11970
Jarvis A, Ouvry G (2019) Essential ingredients for rational drug design. Bioorganic & Medicinal Chemistry Letters p 126674
Jeziorski B, Moszynski R, Szalewicz K (1994) Perturbation theory approach to intermolecular potential energy surfaces of van der waals complexes. Chem Rev 94(7):1887–1930
Kasavajhala K, Bikkina S, Patil I, MacKerell Jr AD, Priyakumar UD (2015) Dispersion interactions between urea and nucleobases contribute to the destabilization of RNA by urea in aqueous solution. J Phys Chem B 119(9):3755–3761
Kauzmann W (1959) Some factors in the interpretation of protein denaturation. In: Advances in Protein Chemistry, vol 14, Elsevier, pp 1–63
Kemmink J, van Mierlo C, Scheek R, Creighton T (1993) Local structure due to an aromatic-amide interaction observed by 1H NMR spectroscopy of peptides related to the n-terminus of bovine pancreatic trypsin inhibitor. J Mol Biol 230:312–322
Kishore B, Terris J, Fernandez-Llama P, Knepper M (1997) Ultramicrodetermination of vasopressin-regulated urea transporter protein in microdissected renal tubules. Am J Physiol Renal Physiol 272(4):F531–F537
Kohn JE, Millett IS, Jacob J, Zagrovic B, Dillon TM, Cingel N, Dothager RS, Seifert S, Thiyagarajan P, Sosnick TR et al (2004) Random-coil behavior and the dimensions of chemically unfolded proteins. Proc Natl Acad Sci USA 101(34):12491–12496
Lambert D, Draper DE (2007) Effects of osmolytes on RNA secondary and tertiary structure stabilities and RNA-mg2+ interactions. J Mol Biol 370(5):993–1005
Lambert D, Draper DE (2012) Denaturation of RNA secondary and tertiary structure by urea: simple unfolded state models and free energy parameters account for measured m-values. Biochem 51(44):9014–9026
Lambert D, Leipply D, Draper DE (2010) The osmolyte tmao stabilizes native RNA tertiary structures in the absence of Mg2+: evidence for a large barrier to folding from phosphate dehydration. J Mol Biol 404(1):138–157
Lauber BS, Hardegger LA, Asraful AK, Lund BA, Dumele O, Harder M, Kuhn B, Engh RA, Diederich F (2016) Addressing the glycine-rich loop of protein kinases by a multi-facetted interaction network: Inhibition of pka and a pkb mimic. Chem: Eur J 22(1):211–221
Lee ME, van der Vegt NF (2006) Does urea denature hydrophobic interactions? J Am Chem Soc 128(15):4948–4949
Lee S, Shek YL, Chalikian TV (2010) Urea interactions with protein groups: a volumetric study. Biopolymers 93(10):866–879
Lee S, Cil O, Diez-Cecilia E, Anderson MO, Verkman AS (2018) Nanomolar-potency 1, 2, 4-triazoloquinoxaline inhibitors of the kidney urea transporter UT-a1. J Med Chem 61(7):3209–3217
LeMoine CMR, Walsh PJ (2015) Evolution of urea transporters in vertebrates: adaptation to urea's multiple roles and metabolic sources. J Exp Biol 218(12):1936–1945. https://doi.org/10.1242/jeb.114223
Levin EJ, Zhou M (2014) Structure of urea transporters. In: Urea Transporters, Springer, pp 65–78
Levin EJ, Quick M, Zhou M (2009) Crystal structure of a bacterial homologue of the kidney urea transporter. Nature 462(7274):757
Levin EJ, Cao Y, Enkavi G, Quick M, Pan Y, Tajkhorshid E, Zhou M (2012) Structure and permeation mechanism of a mammalian urea transporter. Proc Natl Acad Sci USA 109(28):11194–11199
Li M, Tou WI, Zhou H, Li F, Ren H, Chen CYC, Yang B (2014) Developing hypothetical inhibition mechanism of novel urea transporter b inhibitor. Sci Rep 4:5775
Li M, Zhao Y, Zhang S, Xu Y, Sy W, Li Bw, Ran Jh, Li Rt, Yang Bx (2019) A thienopyridine, CB-20, exerts diuretic activity by inhibiting urea transporters. Acta Pharmacol Sin 1
Loschi L, Brokx SJ, Hills TL, Zhang G, Bertero MG, Lovering AL, Weiner JH, Strynadka NCJ (2004) Structural and biochemical identification of a novel bacterial oxidoreductase. J Biol Chem 279(48):50391–50400
Lucien N, Sidoux-Walter F, Roudier N, Ripoche P, Huet M, Trinh-Trang-Tan MM, Cartron JP, Bailly P (2002) Antigenic and functional properties of the human red blood cell urea transporter hUT-b1. J Biol Chem 277(37):34101–34108
Ma H, Proctor DJ, Kierzek E, Kierzek R, Bevilacqua PC, Gruebele M (2006) Exploring the energy landscape of a small RNA hairpin. J Am Chem Soc 128(5):1523–1530
Ma JC, Dougherty DA (1997) The cation- π interaction. Chem Rev 97(5):1303–1324
Macey R (1984) Transport of water and urea in red blood cells. Am J Physiol 246(3):C195–C203
Macias AT, Norton JE, Evanseck JD (2003) Impact of multiple cation-π interactions upon calix [4] arene substrate binding and specificity. J Am Chem Soc 125(8):2351–2360
Mahen EM, Harger JW, Calderon EM, Fedor MJ (2005) Kinetics and thermodynamics make different contributions to RNA folding in vitro and in yeast. Mol Cell 19(1):27–37
Mason PE, Neilson GW, Enderby JE, Saboungi ML, Dempsey CE, MacKerell AD, Brady JW (2004) The structure of aqueous guanidinium chloride solutions. J Am Chem Soc 126(37):11462–11470
Mason PE, Dempsey CE, Vrbka L, Heyda J, Brady JW, Jungwirth P (2009) Specificity of ion- protein interactions: Complementary and competitive effects of tetrapropylammonium, guanidinium, sulfate, and chloride ions. J Phys Chem B 113(10):3227–3234
Mathai JC, Mori S, Smith BL, Preston GM, Mohandas N, Collins M, van Zijl PC, Zeidel ML, Agre P (1996) Functional analysis of aquaporin-1 deficient red cells the colton-null phenotype. J Biol Chem 271(3):1309–1313
Maufrais C, Fazakerley G, Cadet J, Boulard Y (2003) Structural study of DNA duplex containing an n-(2-deoxy-β-d-erythro-pentofuranosyl) formamide frameshift by NMR and restrained molecular dynamics. Nucleic Acids Res 31(20):5930–5940
Mayrand RR, Levitt DG (1983) Urea and ethylene glycol-facilitated transport systems in the human red cell membrane. saturation, competition, and asymmetry. J Gen Physiol 81(2):221–237
McNulty JM, Jerkovic B, Bolton PH, Basu AK (1998) Replication inhibition and miscoding properties of DNA templates containing a site-specific cis-thymine glycol or urea residue. Chem Res Toxicol 11(6):666–673
McNulty R, Ulmschneider JP, Luecke H, Ulmschneider MB (2013) Mechanisms of molecular transport through the urea channel of helicobacter pylori. Nat Commun 4:2900
Merchant KA, Best RB, Louis JM, Gopich IV, Eaton WA (2007) Characterizing the unfolded states of proteins using single-molecule FRET spectroscopy and molecular simulations. Proc Natl Acad Sci USA 104(5):1528–1533
Meyer EA, Castellano RK, Diederich F (2003) Interactions with aromatic rings in chemical and biological recognition. Angew Chem Int Ed 42(11):1210–1250
Miner JC, García AE (2017) Equilibrium denaturation and preferential interactions of an RNA tetraloop with urea. J Phys Chem B 121(15):3734–3746
Moeser B, Horinek D (2013) Unified description of urea denaturation: backbone and side chains contribute equally in the transfer model. J Phys Chem B 118(1):107–114
Müller-Dethlefs K, Hobza P (2000) Noncovalent interactions: a challenge for experiment and theory. Chem Rev 100(1):143–168
Na S, Steinbrecher T, Koslowski T (2018) Thermodynamic integration network approach to ion transport through protein channels: Perspectives and limits. J Comput Chem 39(30):2539–2550

Ni X, Heidenreich D, Christott T, Bennett J, Moustakim M, Brennan PE, Fedorov O, Knapp S, Chaikuad A (2019) Structural insights into interaction mechanisms of alternative piperazine-urea YEATS domain binders in MLLT1. ACS Med Chem Lett

Niedzwiecka A, Marcotrigiano J, Stepinski J, Jankowska-Anyszka M, Wyslouch-Cieszynska A, Dadlez M, Gingras AC, Mak P, Darzynkiewicz E, Sonenberg N et al (2002) Biophysical studies of eIF4e cap-binding protein: recognition of mRNA 5 cap structure and synthetic fragments of eIF4g and 4e-BP1 proteins. J Mol Biol 319(3):615–635

Nordstrom LJ, Clark CA, Andersen B, Champlin SM, Schwinefus JJ (2006) Effect of ethylene glycol, urea, and n-methylated glycines on DNA thermal stability: the role of DNA base pair composition and hydration. Biochem 45(31):9604–9614

O'Brien EP, Dima RI, Brooks B, Thirumalai D (2007) Interactions between hydrophobic and ionic solutes in aqueous guanidinium chloride and urea solutions: lessons for protein denaturation mechanism. J Am Chem Soc 129(23):7346–7353

Onuchic JN, Luthey-Schulten Z, Wolynes PG (1997) Theory of protein folding: the energy landscape perspective. Annu Rev Phys Chem 48(1):545–600

Oostenbrink C, van Gunsteren WF (2005) Methane clustering in explicit water: effect of urea on hydrophobic interactions. Phys Chem Chem Phys 7(1):53–58

Oprzeska-Zingrebe EA, Smiatek J (2018) Preferential binding of urea to single-stranded DNA structures: a molecular dynamics study. Biophyscal J 114(7):1551–1562

Oprzeska-Zingrebe EA, Kohagen M, Kästner J, Smiatek J (2019) Unfolding of DNA by co-solutes: insights from kirkwood–buff integrals and transfer free energies. Eur Phys J Spec Top 227(14):1665–1679

Pace C (1986) Determination and analysis of urea and guanidine hydrochloride denaturation curves. In: Methods in enzymology, vol 131, Academic Press, pp 266–280

Padhi S, Priyakumar UD (2016) Urea–aromatic stacking and concerted urea transport: conserved mechanisms in urea transporters revealed by molecular dynamics. J Chem Theory Comput 12(10):5190–5200

Padhi S, Priyakumar UD (2017) Microsecond simulation of human aquaporin 2 reveals structural determinants of water permeability and selectivity. BBA-Biomembranes 1859(1):10–16

Padhi S, Priyakumar UD (2020) Selectivity and Transport in Aquaporins from Molecular Simulation Studies. Academic Press

Padhi S, Khan N, Jameel S, Priyakumar UD (2013) Molecular dynamics simulations reveal the HIV-1 Vpu transmembrane protein to form stable pentamers. PloS one 8(11):e79779

Padhi S, Ramakrishna S, Priyakumar UD (2015) Prediction of the structures of helical membrane proteins based on a minimum unfavorable contacts approach. J Comput Chem 36(8):539–552

Padhi S, Reddy LK, Priyakumar UD (2017) pH-mediated gating and formate transport mechanism in the escherichia coli formate channel. Mol Simulat 43(13-16):1300–1306

Parrish RM, Sitkoff DF, Cheney DL, Sherrill CD (2017) The surprising importance of peptide bond contacts in drug–protein interactions. Chem: Eur J 23(33):7887–7890

Patra S, Anders C, Erwin N, Winter R (2017) Osmolyte effects on the conformational dynamics of a DNA hairpin at ambient and extreme environmental conditions. Angew Chem 129(18):5127–5131

Pieńko T, Trylska J (2019) Computational methods used to explore transport events in biological systems. J Chem Inf Model 59(5):1772–1781

Pincus DL, Hyeon C, Thirumalai D (2008) Effects of trimethylamine N-oxide (TMAO) and crowding agents on the stability of RNA hairpins. J Am Chem Soc 130(23):7364–7372

Priyakumar UD, Hyeon C, Thirumalai D, MacKerell Jr AD (2009) Urea destabilizes RNA by forming stacking interactions and multiple hydrogen bonds with nucleic acid bases. J Am Chem Soc 131(49):17759–17761

Qiu Z, Kuhn B, Aebi J, Lin X, Ding H, Zhou Z, Xu Z, Xu D, Han L, Liu C et al (2016) Discovery of fluoromethylketone-based peptidomimetics as covalent atg4b (autophagin-1) inhibitors. ACS Med Chem Lett 7(8):802–806

Ramakrishna S, Padhi S, Priyakumar UD (2015) Modeling the structure of SARS 3a transmembrane protein using a minimum unfavorable contact approach. J Chem Sci 127(12):2159–2169

Raunser S, Mathai JC, Abeyrathne PD, Rice AJ, Zeidel ML, Walz T (2009) Oligomeric structure and functional characterization of the urea transporter from actinobacillus pleuropneumoniae. J Mol Biol 387(3):619–627

Record MT, Guinn E, Pegram L, Capp M (2013) Introductory lecture: interpreting and predicting hofmeister salt ion and solute effects on biopolymer and model processes using the solute partitioning model. Faraday Discuss 160:9–44

Riley KE, Hobza P (2012) On the importance and origin of aromatic interactions in chemistry and biodisciplines. Acc Chem Res 46(4):927–936

Riley KE, Pitonák M, Jurecka P, Hobza P (2010) Stabilization and structure calculations for noncovalent interactions in extended molecular systems based on wave function and density functional theories. Chem Rev 110(9):5023–5063

Roehrig S, Straub A, Pohlmann J, Lampe T, Pernerstorfer J, Schlemmer KH, Reinemer P, Perzborn E (2005) Discovery of the novel antithrombotic agent 5-chloro-n-({(5 S)-2-oxo-3-[4-(3-oxomorpholin-4-yl) phenyl]-1, 3-oxazolidin-5-yl} methyl) thiophene-2-carboxamide (bay 59-7939): an oral, direct factor Xa inhibitor. J Med Chem 48(19):5900–5908

Rossky PJ (2008) Protein denaturation by urea: slash and bond. Proc Natl Acad Sci USA 105(44):16825–16826

Rupley J (1964) The effect of urea and amides upon water structure1. J Phys Chem 68(7):2002–2003

Salonen LM, Bucher C, Banner DW, Haap W, Mary JL, Benz J, Kuster O, Seiler P, Schweizer WB, Diederich F (2009) Cation–π interactions at the active site of factor Xa: dramatic enhancement upon stepwise N-alkylation of ammonium ions. Angew Chem Int Ed 48(4):811–814

Salonen LM, Ellermann M, Diederich F (2011) Aromatic rings in chemical and biological recognition: energetics and structures. Angew Chem Int Ed 50(21):4808–4842

Salonen LM, Holland MC, Kaib PS, Haap W, Benz J, Mary JL, Kuster O, Schweizer WB, Banner DW, Diederich F (2012) Molecular recognition at the active site of factor Xa: cation–π interactions, stacking on planar peptide surfaces, and replacement of structural water. Chem: Eur J 18(1):213–222

Sands JM (2003) Mammalian urea transporters. Ann Rev Physiol 65(1):543–566

Sands JM, Knepper MA (1987) Urea permeability of mammalian inner medullary collecting duct system and papillary surface epithelium. J Clin Invest 79(1):138–147

Sarkar K, Meister K, Sethi A, Gruebele M (2009) Fast folding of an RNA tetraloop on a rugged energy landscape detected by a stacking-sensitive probe. Biophys J 97(5):1418–1427

Schafer JA, Troutman SL, Andreoli TE (1974) Osmosis in cortical collecting tubules: Adh-independent osmotic flow rectification. J Gen Physiol 64(2):228–240

Schellman JA (1955a) The stability of hydrogen-bonded peptide structures in aqueous solution. C R Trav Lab Carlsberg Chim 29(14-15):230–259

Schellman JA (1955b) The thermodynamics of urea solutions and the heat of formation of the peptide hydrogen bond. C R Trav Lab Carlsberg Chim 29(14-15):223–229

Schottel BL, Chifotides HT, Dunbar KR (2008) Anion-π interactions. Chem Soc Rev 37:68–83

Schug KA, Lindner W (2005) Noncovalent binding between guanidinium and anionic groups: focus on biological-and synthetic-based arginine/guanidinium interactions with phosph[on]ate and sulf[on]ate residues. Chem Rev 105(1):67–114

Scrutton NS, Raine A (1996) Cation-pi bonding and amino-aromatic interactions in the biomolecular recognition of substituted ammonium ligands. Biochem J 319(Pt 1):1

Sebbane F, Bury-Moné S, Cailliau K, Browaeys-Poly E, De Reuse H, Simonet M (2002) The yersinia pseudotuberculosis yut protein, a new type of urea transporter homologous to eukaryotic channels and functionally interchangeable in vitro with the helicobacter pylori urei protein. Mol Microbiol 45(4):1165–1174

Shelton VM, Sosnick TR, Pan T (1999) Applicability of urea in the thermodynamic analysis of secondary and tertiary RNA folding. Biochem 38(51):16831–16839

Shi Y, Sitkoff D, Zhang J, Klei HE, Kish K, Liu ECK, Hartl KS, Seiler SM, Chang M, Huang C et al (2008) Design, structure- activity relationships, x-ray crystal structure, and energetic contributions of a critical p1 pharmacophore: 3-chloroindole-7-yl-based factor Xa inhibitors. J Med Chem 51(23):7541–7551

Shimizu S, Chan HS (2002) Origins of protein denatured state compactness and hydrophobic clustering in aqueous urea: inferences from nonpolar potentials of mean force. Proteins: Struct Funct Bioinf 49(4):560–566

Smith C, Rousselet G (2001) Facilitative urea transporters. J Membr Biol 183(1):1–14

Smith CP (2009) Mammalian urea transporters. Exp Physiol 94(2):180–185

Sosnick TR (2001) Characterization of tertiary folding of RNA by circular dichroism and urea. Curr Protoc Nucleic Acid Chem 4(1):11–5

Steinke N, Gillams RJ, Pardo LC, Lorenz CD, McLain SE (2016) Atomic scale insights into urea–peptide interactions in solution. Phys Chem Chem Phys 18(5):3862–3870

Street TO, Bolen DW, Rose GD (2006) A molecular mechanism for osmolyte-induced protein stability. Proc Natl Acad Sci USA 103(38):13997–14002

Strugatsky D, McNulty R, Munson K, Chen CK, Soltis SM, Sachs G, Luecke H (2013) Structure of the proton-gated urea channel from the gastric pathogen helicobacter pylori. Nature 493(7431):255

Stumpe MC, Grubmüller H (2007) Interaction of urea with amino acids: implications for urea-induced protein denaturation. J Am Chem Soc 129(51):16126–16131

Stumpe MC, Grubmüller H (2008) Polar or apolar—the role of polarity for urea-induced protein denaturation. PLoS computational biology 4(11):e1000221

Stumpe MC, Grubmüller H (2009) Urea impedes the hydrophobic collapse of partially unfolded proteins. Biophys J 96(9):3744–3752

Su P, Li H (2009) Energy decomposition analysis of covalent bonds and intermolecular interactions. J Chem Phys 131(1):014102

Su P, Jiang Z, Chen Z, Wu W (2014) Energy decomposition scheme based on the generalized kohn–sham scheme. J Phys Chem A 118(13):2531–2542

Su Z, Dias CL (2017) Molecular interactions accounting for protein denaturation by urea. J Mol Liq 228:168–175

Suresh G, Padhi S, Patil I, Priyakumar UD (2016) Urea mimics nucleobases by preserving the helical integrity of b-DNA duplexes via hydrogen bonding and stacking interactions. Biochemistry 55(40):5653–5664

Tanford C (1964) Isothermal unfolding of globular proteins in aqueous urea solutions. J Am Chem Soc 86(10):2050–2059

Tanford C (1970) Protein denaturation: Part c.* theoretical models for the mechanism of denaturation. In: Adv Protein Chem, vol 24, Elsevier, pp 1–95

Thirumalai D, Hyeon C (2005) RNA And protein folding: common themes and variations. Biochem 44(13):4957–4970

Thirumalai D, Woodson S (1996) Kinetics of folding of proteins and RNA. Acc Chem Res 29(9):433–439

Timchenko A, Langowski J, Serdyuk I (1993) Structural changes in 16s RNA from escherichia coli upon unfolding by urea. Biopolymers: Original Research on Biomolecules 33(11):1747–1755

Toupkanloo HA, Rahmani Z (2018) An in-depth study on noncovalent stacking interactions between DNA bases and aromatic drug fragments using dft method and aim analysis: conformers, binding energies, and charge transfer. Appl Biol Chem 61(2):209–226

Tsuzuki S, Honda K, Uchimaru T, Mikami M, Tanabe K (2000a) The magnitude of the CH/π interaction between benzene and some model hydrocarbons. J Am Chem Soc 122(15):3746–3753

Tsuzuki S, Honda K, Uchimaru T, Mikami M, Tanabe K (2000b) Origin of the attraction and directionality of the NH/π interaction: Comparison with OH/π and CH/π interactions. J Am Chem Soc 122(46):11450–11458

Vanommeslaeghe K, Hatcher E, Acharya C, Kundu S, Zhong S, Shim J, Darian E, Guvench O, Lopes P, Vorobyov I, Mackerell AD (2010) Charmm general force field: a force field for drug-like molecules compatible with the charmm all-atom additive biological force fields. J Comput Chem 31(4):671–690

Vanzi F, Madan B, Sharp K (1998) Effect of the protein denaturants urea and guanidinium on water structure: a structural and thermodynamic study. J Am Chem Soc 120(41):10748–10753

Wales D (2003) Energy landscapes: Applications to clusters, biomolecules and glasses. Cambridge University Press

Wallace S (1994) DNA Damages processed by base excision repair: biological consequences. Int J Radiat Biol 66(5):579–589

Wallqvist A, Covell D, Thirumalai D (1998) Hydrophobic interactions in aqueous urea solutions with implications for the mechanism of protein denaturation. J Am Chem Soc 120(2):427–428

Wang Y, Tajkhorshid E (2007) Molecular mechanisms of conduction and selectivity in aquaporin water channels. J Nutr 137(6):1509S–1515S

Wang Y, Wang J, Yao L (2015a) Computational study of peptide plane stacking with polar and ionizable amino acid side chains. J Phys Chem A 119(14):3471–3478

Wang Z, Yu T, Sang JP, Zou XW, Yan C, Zou X (2015b) Computation and simulation of the structural characteristics of the kidney urea transporter and behaviors of urea transport. J Phys Chem B 119(16):5124–5131

Waters ML (2002) Aromatic interactions in model systems. Curr Opin Chem Biol 6(6):736–741

Weeks DL, Gushansky G, Scott DR, Sachs G (2004) Mechanism of proton gating of a urea channel. J Biol Chem 279(11):9944–9950

Weerasinghe S, Smith PE (2003) A kirkwood- buff derived force field for mixtures of urea and water. J Phys Chem B 107(16):3891–3898

Weigend F, Häser M, Patzelt H, Ahlrichs R (1998) Ri-mp2: optimized auxiliary basis sets and demonstration of efficiency. Chem Phys Lett 294(1):143–152

Wheeler SE (2012) Understanding substituent effects in noncovalent interactions involving aromatic rings. Acc Chem Res 46(4):1029–1038

Wilkins DK, Grimshaw SB, Receveur V, Dobson CM, Jones JA, Smith LJ (1999) Hydrodynamic radii of native and denatured proteins measured by pulse field gradient NMR techniques. Biochem 38(50):16424–16431

Yao C, Anderson MO, Zhang J, Yang B, Phuan PW, Verkman A (2012) Triazolothienopyrimidine inhibitors of urea transporter UT-b reduce urine concentration. J Am Soc Nephrol 23(7):1210–1220

Yoon J, Thirumalai D, Hyeon C (2013) Urea-induced denaturation of preq1-riboswitch. J Am Chem Soc 135(32):12112–12121

Zangi R, Zhou R, Berne B (2009) Urea's action on hydrophobic interactions. J Am Chem Soc 131(4):1535–1541

Zhang HT, Wang Z, Yu T, Sang JP, Zou XW, Zou X (2017) Modeling of flux, binding and substitution of urea molecules in the urea transporter dvUT. J Mol Graph and Model 76:504–511

Zhang W, Capp MW, Bond JP, Anderson CF, Record MT (1996) Thermodynamic characterization of interactions of native bovine serum albumin with highly excluded (glycine betaine) and moderately accumulated (urea) solutes by a novel application of vapor pressure osmometry. Biochem 35(32):10506–10516

Zhao D, Sonawane N, Levin MH, Yang B (2007) Comparative transport efficiencies of urea analogues through urea transporter UT-b. Biochim Biophys Acta 1768(7):1815–1821

Zhao Y, Li M, Li B, Zhang S, Su A, Xing Y, Ge Z, Li R, Yang B (2019) Discovery and optimization of thienopyridine derivatives as novel urea transporter inhibitors. Eur J Med Chem 172:131–142

Ziv G, Haran G (2009) Protein folding, protein collapse, and tanford's transfer model: Lessons from single-molecule FRET. J Am Chem Soc 131(8):2942–2947